"A CRISPR-dCas13 RNA-editing tool to study alternative splicing"

Yaiza Núñez-Álvarez[1]*, Tristan Espie--Caullet[1,2], Reini F. Luco[1,2,3]*

1. Institut de Génétique Humaine, Université de Montpellier – CNRS, Montpellier, France. 2. Current address : Institut Curie, PSL Research University, CNRS UMR3348, Orsay, France. 3. Équipe labellisée Ligue contre le cancer.

* Corresponding authors: yaiza.nunez-alvarez@igh.cnrs.fr and reini.luco@igh.cnrs.fr

ABSTRACT

Alternative splicing is an RNA processing used by the cell to increase its protein diversity and genome plasticity through generation of several transcripts from the same gene. It affects the vast majority of biological processes, from stem cell differentiation to cell metabolism. However, tools to properly study the role of a specific splice variant are still missing. With the discovery of the bacterial CRISPR system, a new era in nucleic acid editing has emerged. RNA-directed CRISPR/Cas13 RNAses were recently shown to efficiently target the RNA with higher specificity than Cas9 to the DNA. In this work, we are taking advantage of the catalytic dead mutant dCas13 family member dCasRx to edit alternative splicing patterns in a physiological context. Thanks to our new strategy, isoform-switching splicing changes are easily obtained at endogenous genes without impacting overall gene expression levels. Moreover, we propose a new application for this dCasRx splicing editing system to identify the key regulatory elements involved in the alternative splicing of a given gene. This new approach will increase the RNA toolkit to properly understand the biological impact and regulatory mechanisms of alternative splicing in a given biological process or pathological scenario.

KEYWORDS

Alternative splicing; CRISPR/dCas13, dCasRx; splicing editing; cis-regulatory RNA elements.

INTRODUCTION

More than 90% of human multi-exon genes are alternatively spliced into different mature mRNAs that are translated into different proteins, with different impacts in the cell (1). Exonic and intronic sequences can be included or excluded in the final mRNA molecule prior to translation via exon skipping, intron retention, mutually exclusive exons or alternative 3' and 5' splice site usage (2). Thanks to this pre-mRNA rearrangements, protein domains involved in cellular localization, ligand binding capacity and regulation of enzymatic activity can change, which will affect the protein function (3). Moreover, changes in the final mRNA sequence can introduce premature STOP codons or induce a nonsense-mediated mRNA decay, thus impacting protein levels (3). Such proteomic diversity can be used as an advantage for the cell, or lead to disease. It has been estimated that at least 15% of genetic diseases are caused by mutations in alternative splice sites and/or splicing regulators, and innovative therapies targeting these events are currently in development to treat diseases, such as cancer (4, 5).

While the number of discovered splicing isoforms grows every day thanks to the increase in RNA sequencing depth and improvements in mass spectrometry, the function and biological impact of the vast majority of these newly identified protein isoforms remains unknown. This is in part due to the existence of technical limitations for the accurate study of splicing isoforms. First, small interfering (siRNA) and short hairpin shRNAs can be used to specifically target the alternatively spliced region of interest. However, these strategies have numerous off-target effects and impact overall gene expression levels, resulting in a protein knock-down rather than a shift in splicing isoforms. On the other hand, transduction of the splicing isoform, using expression vectors, results in protein overexpression, which often does not reflect physiological conditions (6). As an alternative, splicing-switching antisense oligonucleotides (SSO) can be designed to specifically target a regulatory region of the pre-mRNA to interfere with recruitment of the splicing machinery and induce a change in the splicing outcome (7). However, this is expensive and difficult to set up, with the need of transfecting high amounts of modified oligonucleotides for an efficient and time-sustained splicing effect, which reduces its feasibility in large scale studies (7). Small molecule splicing modulators, which are synthetic analogues to inhibit splicing reactions, are an innovative new strategy of special interest in the clinic (8). Unfortunately, there are difficult to implement and can lead to many indirect effects. Recently, with the discovery of a unique prokaryotic immune system to eliminate nucleic acid fragments from bacteriophages, called the Clustered Regularly Interspaced Short Palindromic Repeats (CRISPR) (9), key cis-regulatory splicing regions can now be targeted at the DNA level to cause a point mutation (or deletion) at a specific regulatory region that will impact splicing (10–12). However, this approach is limited to the existence of a protospacer adjacent motif (PAM) near the targeted region for Cas9 cleavage, it requires the modification of both alleles and is irreversible, with a considerable number of off-target genomic effects.

In 2016, the discovery of the first RNA-targeting CRISPR-associated family of proteins, called Cas13, opened new perspectives in splicing editing (13, 14). Cas13, and the catalytically inactive dCas13, are RNA-guided RNases that comprise 4 subfamilies: (d)Cas13a, b, c and d. The most efficient Cas13 RNAses are PspCas13b (from *Prevotella*

sp.), PguCas13b (from *Porphyromonas gulae)* and RfxCas13d (from *Ruminococcus flavefaciens*), which will be short named as CasRx for simplicity (15–18). CasRx is one of the smallest Cas13s known up to date, showing a robust and highly specific knock-down activity when targeted against coding and non-coding RNAs (15, 19). Moreover, as the other dCas13 orthologues, it does not require special sequence specificities for RNA targeting, such as protospacer flanking sequences (PFS), except for the presence of uracils in the RNA sequence, making virtually possible to target any RNA (15, 16). The catalytically dead version of CasRx, called dCasRx, was produced by four-point mutations in the nuclease domain (R239A/H244A/R858A/ H863A), which abolished its cleavage capacity without affecting the RNA binding (15). This ability has been largely used to label the RNA with fluorescent proteins fused to dCasRx (20); to modify the RNA by targeting different RNA editing enzymes, such as ADAR (21) or the m6A methyltransferase METLL3 (22); and to modify alternative splicing patterns at majorly splicing minigenes (6, 15, 23). However the use of dCasRx to mediate splicing changes in endogenously expressed genes has been much less extended, even though CasRx has been used to downregulate endogenous mRNAs in human cells, embryos (24, 25), flies (26, 27), zebrafish (28), plants (29), and bacteria (30, 31).

We thus aimed at studying important aspects of dCas13-mediated splicing editing to establish a user-friendly guideline of how to induce the strongest changes in alternative splicing at a specific gene. Different gRNA design tools were compared, with different gRNA lengths and positions along the exon for an optimal shift in splicing isoforms, and all our gRNAs were tested in endogenous genes, proving its functionality in a physiological context. Finally, limitations for the splicing editing were observed and discussed, and a new application for dCasRx targeting is proposed for identification of key cis-regulatory RNA regions for splicing modulation.

MATERIAL AND METHODS

Cell culture of human cell lines

Human Embryonic Kidney (HEK) cell line 293T and HCT116 cells were maintained at 37°C with 5% CO_2 in DMEM (4.5 g/L glucose) with Glutamax, supplemented with 10% FBS (Heat inactivated Sigma F9665-500ML) and 1% penicillin/streptomycin. Cells were maintained in subconfluent conditions and passaged at 1:10 ratio each 3 days. HEK293T cell line was a kindly gift by (Dr. Nadine Laguette) and HCT116 was a gift of Dr. Hervé Seitz lab and were not otherwise authenticated but periodically tested for mycoplasma.

Cloning and Plasmids

To allow indirect quantification of gRNA expression, pXR003 processed gRNA was cloned into pKLV2.3-Hygro mCherry gRNA lentiviral plasmid (33) using EcoRI and Mlu and amplying (d)CasRx directed repeats from pXR003 processed gRNA (Addgene #109053) using the following F (CCCACGCGTGAGGGCCTATTTCCCATGATTC) and R primers (CCCCCGAATTC AAAAAAAAGGTCTTCTCGAAGACC).

Transient transfection of human cell lines

For mRNA expression analysis, HEK293T and HCT116 cells were plated at a density of 20,000 cells per well in a 96-well plate and transfected with 200 ng of Cas13 expression

plasmid and 200 ng of gRNA expression plasmid using Lipofectamine 2000 (Life Technologies) according to the manufacturer's protocol DMEM (4.5 g/L glucose) with Glutamax, supplemented with 10% FBS (Heat inactivated Sigma F9665-500ML) without penicillin/streptomycin. Transfected cells were harvested 72 hours post-transfection.

For protein expression analysis, HEK293T cells were plated at a density of 200,000 cells per well in a 24-well plate and transfected with 800 ng of dCasRx expression plasmid and 800 ng of gRNA expression plasmid using Lipofectamine 2000 (Life Technologies) according to the manufacturer's protocol in HEK media without penicillin/streptomycin. Transfected cells were harvested 72 hours post-transfection.

gRNA design

For custom tilling gRNA design none special requirements were taken into account besides being located in the antisense DNA strand of the corresponding gene and trying to cover the exons selected with the minimum number of gRNAs.

For gRNA design using "cas13design" software, it was selected the most abundant isoform expressed in HEK293T which included the alternative spliced exon of interest. For the top scored gRNA, only the best top scored was selected. When several top scored gRNAs were used, they were selected the top scored ones showing no overlapping between them. The gRNAs designed with this software are annotated as "CD".

CHOPCHOP Homo sapiens hg38 genome version, using "CRISPR/Cpf1 or CasX" option without any PAM requirements. The gRNAs designed with this software are annotated as "CC".

In all cases, gRNA annotation was done from acceptor to donor, regardless of the strand of the gene. When both intronic and exonic regions were targeted with different gRNAs along the same pre-mRNA, we labelled the gRNAs as "iX" for intronic and "eX" for exonic. gRNAs located in acceptor and donor regions were labelled as "Acc" or "Don", respectively.

gRNA cloning

gRNAs were ordered desalted and resuspended to 100 µM oligonucleotides at Eurofins Genomics with the corresponding overhanging BbsI complementary sites as indicated in Table 2 for (d)CasRx gRNAs and in Table 3 for (d)Cas13b gRNAs. gRNAs were annealed in (1 µl Forward primer, 1 µl Reverse primer, 5 µl Buffer 4 NEB, 43 µl H2O) by heating at 98 °C for 5 min and allowing the tubes to cool down to room temperature in the thermoblock (~3h). 3µl of annealed oligonucleotides were ligated with 50ng of gRNA backbone vector (previously cut with BbsI-HF and gel extracted) using Quick Ligation kit (M2200S, NewEngland Biolabs) and transformed into NEB 5-alpha Competent E. coli (C2987I, NewEnglandBiolabs). Colonies were screened by PCR screening using GoTaq G2 Hot Start green Master Mix (M7422, Promega) using the consensus pLKO F oligonucleotide (5'->3'GACTATCATATGCTTACCGT) and the corresponding reverse primer used to clone the gRNA in a final volume of 12,5 µl using the following program: 95°C_2min, 30x(95°C_30", 54°C_30", 72°C_10"), 72°C_2min.

shRNA cloning and splicing factor knock-down

pLKO.1-blast was digested using AgeI-HF and EcoRI-HF enzymes and vector was cut and purified from 1% agarose gel. shRNAs were ordered as oligonucleotides with the

corresponding overhanging sequences (Table 5), annealed and cloned as explained for gRNAs in "gRNA cloning".

For PTB, RbFOX2, SRSF1, MBNL1, FUS, ELAV1, CELF1 and KHDRBS3 knock-down, HEK393T cells were plated at $2.5x10^6$ cells / 100mm dish. Cells were transfected with 5µg of the shRNA plasmid of interest, 250mM $Cacl_2$, qsp 500µL sterile water. Samples were gently mixed and completed with 2X HEPES Buffered Saline (HBS), Incubated 10 min at room temperature. Mixes were dropped on HEK293T and cells were maintained at 37°C with 5% CO_2 (Day 2). 16h after transfection medium was replaced and HEK293T cells were collected for RNA expression 72h after transfection. For SRSF3 knock-down, HEK293T cells were plated in 96 well plates and transfected with 200ng of SRSF3 or SHC002 shRNA vectors as explained in "Transient transfection of human cell lines". Cells were collected 72h after transfection and RNA was extracted using TurboCapture 96 mRNA Kit (QIAGEN) following manufacturer's protocol.

Gene expression and exon splicing analysis

Cells were lysed 72 hours post-transfection by directly adding 35 µl of β-mercaptoethanol-supplemented TCL buffer to wells and mRNA was extracted using TurboCapture 96 mRNA Kit (QIAGEN) following manufacturer's protocol. Captured mRNA was eluted by adding 11 µl of TCE buffer and incubating at 65 ºC for 5 min. All 11 µl eluted mRNA were reverse transcribed using random hexamer primers and Transcriptor First Strand cDNA Synthesis Kit (Roche) at 65°C for 10 min, 25°C for 10 min, 50°C for 60 min, and 85°C for 5 min. Then, cDNA was diluted 1/5 and analyzed by RT-qPCR using 2X iTaq Universal Sybr Green Supermix (Bio-Rad) and the oligonucleotides indicated in Table S2. qPCR was carried out in 10 µL reactions and technical duplicates in 96 well-plates using CFX96 Touch Real-Time PCR Instruments (Bio-Rad).

Primers were design whenever possible between exons spanning an intron to avoid unespliced isoform quantification using IDT Realtime PCR Tool and Primer3 softwares. Primers for total gene expression analysis were designed between constitutive exons far from the targeted alternative spliced exon to avoid quantification of knock-down of only the isoforms containing the alternative spliced exon instead of total gene knock-down, and to avoid possible confusing sterically splicing effects of CasRx. Total gene expression analysis was calculated using 2^(ΔCt) method and TBP as reference gene. Splicing inclusion was calculated using the same method by comparing the Ct of the corresponding alternative spliced exon to the corresponding total gene expression level. Inclusion level goes from 0 to 1, indicating 0 none inclusion of the alternative spliced exon and 1 a 100% inclusion of the exon in all isoforms. To make gene expression or exon inclusion relative to gRNA NT2, the corresponding normalized data as mentioned was divided by the corresponding value of matching gRNA NT2 transfected condition. Thus, a relative value of 1 indicates no change respect to the non-targeting condition, while <1 values indicate mRNA downregulation for "Relative abundance" or exon exclusion for "Exon relative inclusion". Values >1 indicate mRNA upregulation for "Relative abundance" or increased exon inclusion for "Exon relative inclusion".

Western blot analysis of PKM isoforms

Cells were lysed in RIPA buffer containing 1X protease inhibitors (cOmplete, 11836145001, Sigma) and quantified using BCA method (BCA Protein Assay, 23227, Pierce). 40 µg of protein/sample were run at 200mV for 1h30 using XCell SureLock Mini-

Cell System (ThermoFisher). NuPAGE 4-12% Bis Tris gels (NP0322B0X, Invitrogen) were Transferred in the same system at 65mV for 1h. Membranes were cut according to protein weight to allow the analysis of the target isoforms and loading controls in the same membrane. Membranes were blocked with 5% w/v BSA in 1x TBS-Tween for 1h and then incubated with the corresponding primary antibodies diluted in blocking buffer o/n at 4°C with shacking. After incubation with the appropriate secondary antibodies, membranes were incubated with ECL Supersignal West Pico Chemiluminescent Substrate (34080, ThermoFisher) and signal was detected using Chemidoc Gel Imaging System (Bio-rad).

RNA Motif search analysis

RNA binding motif search analysis was done using CTNND1 exon2 sequence in four public software: RBPDB v1.3 (http://rbpdb.ccbr.utoronto.ca), RBPMAP v1.1 (http://rbpmap.technion.ac.il), SFMAP v1.8 (http://sfmap.technion.ac.il/), Spliceaid (http://www.introni.it/splicing.html). All software were used with the default parameter settings, except for some exceptions. For RBPDB the threshold 0.8 was applied. For RBPMAP, the Stringency level used was “High stringency” with all motifs available from Human/mouse. For SFMAP both “Perfect match” and “High stringency” stringency levels were used. We have represented motifs predicted by at least 2/4 software.

Quantification and Statistical Analysis

All values are depicted as mean ± SD and individual replicates are plotted as dots. For comparing two groups, a two-tailed Student’s t test was used. P values were plotted only if the comparison to gRNA NT1 and NT2 were both significant in independent t-tests. For multiple comparisons, one-way ANOVA with Dunnett multiple comparison correction was used to assess statistical significance of transcript changes using GraphPad Prism 9. At least three biological replicates were used for each experiment, as plotted and indicated specifically in each figure. (43)

RESULTS AND DISCUSSION

A position-dependent effect for dCasRx-mediated modulation of splicing.

It was previously shown that targeting of dCasRx to regulatory splice sites flanking the alternatively spliced exon, such as the branch point or the donor and acceptor sites, could induce exon skipping, which is the exclusion of the exon from the mature mRNA (15). Best splicing editing results were obtained when using a combination of gRNAs or fusing the effector domain of the splicing repressor hnRNPA1 to the dCasRx protein (15). Since most of these gRNAs were tested in splicing minigenes, we aimed at elucidating the real impact of dCasRx in endogenous genes.

We first targeted dCasRx to the alternatively spliced exon 2 of the catenin delta-1 gene (*CTNND1*.Ex2*)*, which is 42% included in HEK293T cells (Percent Spliced In - PSI=0.42, Supplementary Figure 1A). Inclusion of exons 2 and 3 changes the translation-initiation start site of CTNND1, which impacts its capacity to interact with E-cadherins, causing destabilization of cell-cell interactions and an increase in the cell’s motility (32).

Moreover, we have recently shown that changes in *CTNND1*.Ex2 splicing have a direct impact in epithelial cells migration and invasiveness (33), which increases the interest of developing efficient tools to induce exon 2 skipping in highly invasive cancer cells. Contrary to what was published in splicing minigenes, neither targeting of the acceptor nor the donor splice site with specific gRNAs had an impact on *CTNND1*.Ex2 splicing (Figure 1A, B). However, the tilling of six gRNAs with 5nt overlap between each other to cover the whole alternatively spliced exon showed that one gRNA (gRNA_e2) was capable of reducing exon 2 inclusion up to 83% (from 42% inclusion to 7%) (Figure 1A-B and Supplementary Figure 1A). While a gRNA immediately upstream of gRNA_e2, gRNA_e1, had a minor impact on exon 2 splicing (~35% reduction). Of note, none of these gRNAs impacted *CTNND1* overall gene expression levels, suggesting a splicing-specific effect (Figure 1C).

To better understand the differences observed in splicing editing when using different gRNAs, we measured the RNA cleavage efficiency of the catalytically active CasRx protein as a reflection of the capacity of the gRNA to properly target CasRx/dCasRx to the pre-mRNA. Even though gRNA_e1 and gRNA_e2 were the only gRNAs inducing a change in splicing, 5 different gRNAs reduced *CTNND1* mRNA levels more than 30%, being gRNA_e6 the most efficient with a 50% knock-down (Figure 1D). Of note, *CTNND1* expression levels were assessed with primers amplifying two constitutive exons downstream exon 2 (exon 6 and 7), not to confuse changes in total mRNA levels with changes in exon 2 splicing. These results suggest that most of these gRNAs have similar RNA targeting efficiencies, but only dCasRx recruitment to a specific location along the exon can impact splicing.

It was surprising that gRNAs targeting the acceptor and donor sites barely impacted *CTNND1* mRNA levels nor splicing (Figure 1B, D). Since these gRNAs have more than 50% of their sequence located in the intronic region, we hypothesized that targeting introns could be less efficient recruiting dCasRx/CasRx than targeting exons. Six more gRNAs were designed in the intronic region downstream exon 2 (Supplementary Figure 1B). None of them impacted splicing nor *CTNND1* overall mRNA levels, supporting our hypothesis (Supplementary Figure 1C-E). In fact, differences in RNA cleavage have also been observed in Cas13 screenings with exon targeting been the most efficient to induce a knock-down (17). However, changes in alternative splicing have successfully been obtained targeting both regions in splicing minigenes (6, 23). It is possible that the existence of secondary and tertiary stem loop structures and/or repeating sequences at full length intronic regions in endogenously spliced genes prevent gRNA accessibility, and thus dCasRx/CasRx editing of the pre-mRNA.

dCasRx is the dCas13 of choice for splicing editing.

There are several Cas13 subfamilies that have been described to successfully induce mRNA degradation (15–18). However, not much is known regarding their catalytically inactive counterparts. For instance, dLwaCas13a was described to reduce just 19% the exon inclusion levels of the studied splicing minigene, in contrast to a 57% reduction when using dCasRx (15). Whereas the catalytic inactive dPspCas13b was recently found to be the dCas13 of choice for RNA imaging (20). We thus aimed at comparing the

splicing editing capacity of different dCas13 proteins known to efficiently target the RNA. Neither dPspCas13b nor dPguCas13b had an impact on *CTNND1*.Ex2 splicing (Supplementary Figure 1F-G, I-J). Although their enzymatically active version did cleave *CTNND1* mRNA to a level comparable to that seen for CasRx (~30-45% reduction in mRNA abundance, Figure 1D and Supplementary Figure 1H), suggesting that dCasRx is the dCas13 of choice to edit alternative splicing. In fact, dCasRx is the smallest protein of the three dCas13 tested (dCasRx is 966 aa, dPspCas13: 1,089 aa and dPguCas13: 1174 aa), which could impact the protein's accessibility to the co-transcriptionally spliced pre-mRNA.

Neither gRNA extension nor increasing gRNA/dCasRx expression levels dramatically improves splicing editing efficiency.

To improve CasRx knock-down efficiency, it was recently reported that an extension of the preconized 22nt gRNA length to 30nt could impact CasRx cleavage capacity (17). We tried such strategy by extending 7nt upstream (5') or downstream (3') some of the gRNAs tested in *CTNND1*.Ex2 (Figure 1E). Such gRNAs were selected based on their cleavage and splicing editing capacity before the extension, with gRNA_e6 selected as the best gRNA for RNA cleavage, gRNA_e2 as the best gRNA for splicing editing and gRNA_e4 as a gRNA with no effect on *CTNND1* splicing (Figure 1B,D). gRNA extension improved CasRx cleavage efficiency in most of the cases up to 50% reduction in *CTNND1* mRNA abundance (Figure 1H). However, only the 5' extension of gRNA_e6 improved dCasRx-mediated splicing editing to a 50% reduction in exon inclusion. While extension of gRNA_e4 did not have an effect on splicing, and gRNA_e2 3' extension even decreased the gRNA's splicing editing efficiency. These results suggest that gRNA extension improves CasRx cleavage efficiency, but does not systematically improve dCasRx splicing effect and can even be deleterious, with only 1 extension out of 6 improving splicing editing (Figure 1B,F).

Another possible limitation to an efficient splicing editing is the necessity for high quantities of dCasRx and/or gRNA to target all pre-mRNA molecules in the nucleus. To test this, we transfected increasing levels of CasRx, dCasRx and gRNA plasmid in HEK293T cells (Supplementary Figure 2). We used gRNA_e1 and gRNA_e2 as the two gRNAs impacting *CTNND1* splicing. We first confirmed that transfection of the gRNA alone cannot impact splicing, nor mRNA levels, supporting a dCasRx-mediated effect (Supplementary Figure 2A-F). Increasing CasRx, dCasRx or gRNA levels (assessed indirectly as mCherry levels, which is expressed in the same plasmid) did not significantly improve RNA cleavage nor splicing, suggesting that higher quantities of CRISPR-associated protein or gRNA are not necessary for an efficient RNA editing (Supplementary Figure 2C,F,I).

In conclusion, dCasRx can efficiently induce isoform-switching splicing changes in an endogenous gene without impacting overall gene expression levels. However, not all the tested gRNAs had the same effect on splicing, despite an impact on RNA cleavage when targeting CasRx, raising the question how to design the best splicing editing gRNA.

Tilling arrays of gRNAs predicted with the "Cas13design" web tool is the best strategy to identify strong splicing editing gRNAs.

There are currently several web tools to design optimal gRNAs for Cas13-mediated RNA knock-down. However, these tools have not been tried yet for their splicing editing capacity when targeting the catalytically dead mutant dCasRx. We thus tested, in our model gene *CTNND1,* two programs used in Cas13 editing: CHOPCHOP (CC) (34) and Cas13design (CD) (17). CHOPCHOP can be used to design gRNAs for several Cas13 family members, whereas Cas13design tool is specific for CasRx. Both web tools calculate RNA accessibility using different methods and look for potential off-targets across the transcriptome for an increased specificity. Cas13design also takes in consideration gRNA-RNA hybridization energy, nucleotide preferences, crRNA folding and the gRNA length (defined as 23nt by default) (17).

The two non-overlapping gRNAs targeting *CTNND1*.Ex2 with highest score from each web tool were compared to our custom designed gRNAs (Figure 1I-L). Web tool-designed gRNAs, specially Cas13design gRNAs (gRNA_CD), had stronger RNA cleavage capacities when using CasRx than our custom gRNAs (compare Figure 1D to Figure 1L, ~45% vs ~62%). However, at the splicing level, Cas13design gRNAs were more efficient than CHOPCHOP gRNAs and comparable to our best editing gRNA (gRNA_e2) (Figure 1B,J).

To test dCasRx capacity to edit splicing at physiologically relevant levels when designing gRNAs with the Cas13design tool, we targeted 12 endogenously expressed genes in HEK293T cells with different gene expression and exon inclusion levels (Figure 2C-E). The highest scored gRNA for each alternatively spliced exon was tested for its capacity to edit splicing and mRNA levels using dCasRx and CasRx, respectively (Figure 2A,B). 8 out of 12 gRNAs significantly changed exon inclusion levels more than 40% (Figure 2A). While almost all gRNAs significantly reduced more than 50% mRNA expression levels when targeting the catalytically active CasRx (Figure 2B). There was no correlation between exon size and the chances of designing an efficient splicing-editing gRNA (Figure 2D). However, we did observe that despite targeting exons already lowly included in HEK293 cells, like *EVI5L*.Ex11, *SPAG9*.Ex24 or *FLNB*.Ex30 (Figure 2C), dCasRx never increased the inclusion levels of any of these exons. On the contrary, it excluded them even more (Figure 2A, the inclusion levels relative to NT2 control are <1).

To test gRNA's position-effect in splicing, we designed tilling arrays of Cas13design gRNAs (Figure 2F-M) and custom designed gRNAs (Supplementary Figure 3A-J) along four of the previously tested exons. We found that even though most of these gRNAs efficiently cleaved the RNA when targeting CasRx, it was not the case for alternative splicing. For instance, in the case of *ARHGEF11*, the gRNA reducing the most mRNA levels (gRNA_CD1) was not impacting splicing when targeting dCasRx. On the contrary, it was a gRNA not cutting the RNA (gRNA_CD3) which impacted the most *ARHGEF11* splicing (Figure 2K,M). While in the case of *SCRIB* and *PLOD2*, even though all the designed gRNAs impacted RNA abundance, only specific gRNAs induced a more than 50% change in splicing (gRNA_CD2 for *SCRIB* and gRNA_CD for *PLOD2*, Figure 2G,I and Supplementary Figure 3B). These results suggest that contrary to CasRx RNA cleavage,

to efficiently impact splicing the gRNA has to target a specific region along the alternatively spliced exon.

Since for *CTNND1*.ex3, which is a very long exon of 289 bp, we could not identify an efficient gRNA, we tried to combine high scored Cas13design splicing-editing gRNAs to increase splicing editing (Supplementary Figure 3E-J). A modest improvement was observed when combining the best splicing editing gRNAs CD3+CD4, suggesting that using more than one gRNA does not significantly improve splicing editing when using suboptimal gRNAs (Supplementary Figure 3F,I).

In conclusion, we confirm the generality of dCasRx as an efficient tool to induce isoform-switching changes in alternative splicing of endogenously expressed RNAs. In our hands, the use of a single gRNA is sufficient to induce a strong splicing change. However, since we observed a position-dependent effect, we recommend to cover the whole exon with a tilling array of highest scored gRNAs from the Cas13design web tool to select the gRNAs with the strongest splicing editing efficiency. From these tilling arrays, we observed that specific gRNAs, sharing common positions along the exon, as in *CTNND1* (gRNA_e2 and CD1) and *SCRIB* (gRNA_CD1 and CD2), had stronger splicing effects than other gRNAs (Figure 1B,J and 2G). We thus next aimed at addressing the functional impact of this position-dependent splicing effect.

dCasRx position-dependent splicing effect points to the existence of cis-regulatory elements at the targeted exon.

It was suggested that recruitment of dCasRx to regulatory splice sites, such as the acceptor and donor sites, would induce splicing changes by interfering with recruitment of the splicing machinery (15, 23). We thus hypothesized whether gRNA's position-dependent effect could reflect the existence of key cis-regulatory regions important for alternative splicing regulation by impacting 3D RNA structures and/or recruitment of the splicing regulators to the pre-mRNA.

To test this, we targeted an alternatively spliced exon extensively characterized thanks to serial sequence deletions in splicing minigenes, which is *CD46*.Ex13, a gene important for the immune system (35). This 93-bp exon is regulated by two strong exonic splicing enhancers (ESE), two exonic silencers (ESS) and several intronic silencers (ISS) and enhancers (ISE) (Figure 3A). We targeted each of these key regulatory regions with high scored gRNAs from the Cas13design tool. As expected, the gRNAs targeting the two exonic splicing enhancers (gRNA_e1, e2, e4) reduced *CD46.*Ex13 inclusion levels more than 50%, with a stronger effect when targeting ESE1 (~70%) than ESE2 (~50%), which is surrounded by splicing silencers and those could be impacting both regions. In fact, the gRNA targeting an exonic splicing silencer (gRNA_e3) significantly increased exon inclusion levels, although modestly from 80% to 90% inclusion (Supplementary Figure 3K). Greater effects are expected in cell lines with a less included exon. However, same as in *CTNND1*, targeting of intronic splicing silencers (gRNA_i3, i4) or enhancers (gRNA_i1), had no effect on *CD46* splicing. These results support our hypothesis that dCasRx impacts alternative splicing by interfering with recruitment of key splicing regulators, activators or repressors, to strong cis-regulatory sequence along the pre-mRNA, with a preference for exonic over intronic regions.

Since we could only increase exon inclusion levels when targeting a well-known splicing silencer present at the exon of *CD46* locus (Figure 3), we targeted an alternatively spliced pre-mRNA, *USP5*, in which a repressive PTB-binding site has been described at the alternative 5'splice site of exon 15 (Supplementary Figure 3L). None of the three gRNAs targeting PTB binding site had an impact on *USP5* alternative splicing, even though PTB knock-down did increase inclusion of the long isoform (*USP5-XL*) (Supplementary Figure 3L-Q). When looking at CasRx cutting activity using these same gRNAs, we observed a low impact in *USP5* mRNA abundance (<20%, Supplementary Figure 3O). These results support our previous observations that targeting intronic regions is not efficiently editing the RNA (for cleavage nor splicing) (Figure 1D, 3D and Supplementary Figure 1E and 3O).

In conclusion, by targeting key cis-regulatory RNA elements, particularly exonic splicing enhancers or silencers, dCasRx can lead to exon skipping or increased inclusion, respectively, by most likely interfering with recruitment of the splicing regulators. Of note, small splicing effects have also been observed by other teams when targeting dCasRx to repressive splicing silencers (23). Since splicing repressor's binding sites are usually present at intronic sequences, and in more than one site along the regulated exon, it is probably difficult to target them all to induce exon inclusion (reviewed in (36). Of note, when dCasRx was fused to the activator domain of well-known splicing factors, such as RBFOX1, it could strongly increase exon inclusion levels at both splicing minigenes and an endogenous gene (6). Best results were obtained when targeting the artificial CRISPR splicing factor to multiple sites nearby the exon. Robust induction of exon inclusion is thus possible, but using more than one gRNA and with a dCasRx fusion protein, which could have indirect effects linked to overexpression of the splicing catalytic domain.

dCasRx splicing editing can be used to identify key regulatory mechanisms.

Classically, splicing regulatory regions, and their associated splicing factors, have been identified by deleting or mutating the RNA binding sites in splicing reporter minigenes (35). Unfortunately, such systems do not often reflect the complexity of an endogenously expressed gene with long flanking intronic regions. Splicing-editing gRNAs should point to the existence of these regulatory binding sites without the need for DNA sequence editing for mechanistic analysis. To test this hypothesis, we first did a gRNA tilling of an exon whose splicing regulators are well known, which is exon 10 from Muscle Piruvate Kinase (*PKM*.Ex10). PKM is a glycolytic enzyme that is spliced into two isoforms. PKM1, which includes exon 9, is expressed in non-proliferative cells, and PKM2, which includes exon 10, is highly expressed in proliferative and cancer cells (37). These two exons are mutually exclusive and influence the transition from aerobic respiration to glycolysis, which confers growth advantage to highly metabolic cancer cells (37).

Upon a tilling array of custom designed gRNAs to cover *PKM*.E10, including the acceptor splice site, only one gRNA had a splicing effect on the gene (gRNA_1, Figure 4A-C). However, instead of inducing exon 10 skipping, it induced exon 9 inclusion. This splicing effect improved x2.5-fold when using the highest scored gRNA from the Cas13design

tool that happened to overlap gRNA_1 (gRNA_CD, Figure 4A,C). These changes in exon inclusion were observed at the mRNA and protein level thanks to the use of splicing-specific antibodies only recognizing the protein isoform including exon 9 (Figure 4E and Supplementary Figure 4A-C). Of note, it has already been reported that targeting exon 10 with antisense oligonucleotides can induce exon 9 inclusion (39) and this dCasRx-mediated splicing effect was specific to PKM since none of the other alternatively spliced genes analysed were impacted (Supplementary Figure 4D-W). Finally, using SpliceAid, a database of human RNA target motifs (38), we identified a strong RNA binding motif for the splicing activator SRSF3 right at the exonic region targeted by the two gRNAs impacting splicing (Figure 4A,C). SRSF3 was previously reported to impact *PKM*.Ex9 splicing (39–41). As expected, and comparable to gRNA_1 and gRNA_CD-mediated splicing effect, SRSF3 knock-down in HEK293T cells confirmed SRSF3 splicing effect on *PKM*.Ex9 despite targeting *PKM*.Ex10 (Figure 4F and Supplementary Figure 4X-Y). Furthermore, this splicing effect was not only observed in HEK293T cells, but also in the colorectal cancer cell line HCT116 (Figure 4G), where SRSF3 has also been described to regulate *PKM* splicing in the same manner (41). These results validate the hypothesis that the position-dependent effect of dCasRx in alternative splicing can help elucidate key regulatory mechanisms that should be further addressed with appropriate analysis.

To further support dCasRx new application in identifying key regulatory splicing mechanisms, we looked for RNA motifs along our model exon *CTNND1*.ex2. Only motifs found in at least two of the four web tools used for motif search analysis were kept (Figure 5A). We first observed a high density of motifs precisely at the regions targeted by the gRNAs impacting splicing (gRNA_e1, e2 and CD1, Figure 1A-B and Figure 5A). shRNA knock-down of the predicted splicing regulators pointed to a regulatory role for SRSF1 and MBNL1 in enhancing splicing, which were motifs precisely enriched at RNA regions targeted by splicing-editing gRNAs, such as gRNA_e1 and gRNA_e2 (Figure 5A-C). However, downregulation of any of these splicing regulators, individually or in combination such as the double knock down of the two splicing factors impacting the most *CTNND1*.Ex2 inclusion (SRSF1 and MBNL1, Figure 5C), had a modest splicing effect compared to the targeting of dCasRx (30-35% vs 80% reduction in exon inclusion, respectively, Figure 1B and 5B). These results suggest that dCasRx targeting to a cis-regulatory region might interfere with the recruitment of several splicing regulators, predicted or not from the RNA motif assay, which would increase its splicing impact and reduce potential compensatory effects from redundant factors in shRNA knock-down assays. Furthermore, with dCasRx we can impact the splicing of our exon of choice without the need to identify the key splicing regulators involved, which is often time-consuming and difficult to reach.

dCasRx is thus an efficient tool to test the physiological impact of editing alternative splicing levels that can also be used to identify key regulatory RNA elements for mechanistic analysis.

CONCLUSION

We have successfully induced more than 50% reduction in exon inclusion levels of 75% of the tested alternatively spliced genes without impacting overall gene expression

levels and using just one gRNA per exon. dCasRx is a cost-effective strategy, easy to implement, that can induce a physiologically relevant splicing shift at the RNA and protein level. For best results, we propose to perform a tilling array of gRNAs along the studied exons, designed with the Cas13design web tool to optimize gRNA's accessibility, which will identify the best editing gRNA. Given that the average cassette exon length in humans is 98 bp (42), 5 sgRNAs should be sufficient to cover the whole exon. With such strategy, not only the best splicing editing effect will be obtained, but it will also underline key cis-regulatory RNA elements to narrow down the splicing regulators involved in more mechanistic assays. Finally, dCasRx pre-mRNA splicing editing does not introduce a permanent change in the genome, as would do a Cas9-mediated mutation of a splicing regulatory region, which is an added value when designing therapeutic strategies to correct a pathological mis-splicing.

As a caveat, dCasRx method is efficient mostly in HEK293T cells, in which high transfection levels are obtained. Splicing editing effects were also observed in HCT116 cells, although with a minor effect. Finally, despite several attempts, and in line with results from other colleagues (6), we could not efficiently induce exon inclusion by just targeting dCasRx. Fusion with splicing regulators' active domains has been proposed as an alternative. Although it has limited effects depending where the fused dCasRx is targeted, and it requires the transfection of several gRNAs, which can increase the number of off-target effects. Improvements in RNA-targeting CRISPR editing tools will open new perspectives in the study of mRNA splicing and its impact in disease.

FUNDING:
This work was supported by the French National Research Agency program Labex EpiGenMed (ANR-Labex) and the Institut National du Cancer (INCa PLBIO grant 2018-146). The "Institut de Génétique Humaine" is supported by the Centre National de la Recherche Scientifique (CNRS) and the University of Montpellier (UM).

ACKNOWLEDGEMENTS
We thank Dr. Maria Moriel-Carretero for her very insightful comments about the manuscript. Dr. Laguette (IGH, Montpellier) and Dr. Seitz (IGH, Montpellier) for HEK293T and HCTT116 cell lines, respectively. Dr. Patrick Hsu (Salk, US) for providing us the plasmids of CasRx, dCasRx and processed gRNA through Addgene. We thank Dr. Ling-Ling Chen Lab (State Key Laboratory of Molecular Biology, Shanghai Institute of Biochemistry and Cell Biology, China.) for providing us the plasmids for PspCas13b, dPspCas13b, dPguCas13b and crRNA backbone.

Competing interests: No competing interests.

REFERENCES

1. Pan,Q., Shai,O., Lee,L.J., Frey,B.J. and Blencowe,B.J. (2008) Deep surveying of alternative splicing complexity in the human transcriptome by high-throughput

sequencing. *Nat. Genet.*, **40**, 1413–1415.
2. Papasaikas,P. and Valcárcel,J. (2016) The Spliceosome: The Ultimate RNA Chaperone and Sculptor. *Trends Biochem. Sci.*, **41**, 33–45.
3. Sulakhe,D., D'Souza,M., Wang,S., Balasubramanian,S., Athri,P., Xie,B., Canzar,S., Agam,G., Gilliam,T.C. and Maltsev,N. (2019) Exploring the functional impact of alternative splicing on human protein isoforms using available annotation sources. *Brief. Bioinform.*, **20**, 1754–1768.
4. Hammond,S.M. and Wood,M.J.A. (2011) Genetic therapies for RNA mis-splicing diseases. *Trends Genet.*, **27**, 196–205.
5. Wang,B.-D. and Lee,N. (2018) Aberrant RNA Splicing in Cancer and Drug Resistance. *Cancers (Basel).*, **10**, 458.
6. Du,M., Jillette,N., Zhu,J.J., Sheng,L. and Cheng,A.W. (2020) CRISPR artificial splicing factors. *Nat. Commun.*, **11**, 1–11.
7. Havens,M.A. and Hastings,M.L. (2016) Splice-switching antisense oligonucleotides as therapeutic drugs. *Nucleic Acids Res.*, **44**, 6549–6563.
8. Schneider-Poetsch,T., Chhipi-Shrestha,J.K. and Yoshida,M. (2021) Splicing modulators: on the way from nature to clinic. *J. Antibiot. (Tokyo).*, **74**, 603–616.
9. Mojica,F.J.M., Díez-Villaseñor,C., García-Martínez,J. and Soria,E. (2005) Intervening sequences of regularly spaced prokaryotic repeats derive from foreign genetic elements. *J. Mol. Evol.*, **60**, 174–182.
10. Tang,J.-X., Chen,D., Deng,S.-L., Li,J., Li,Y., Fu,Z., Wang,X.-X., Zhang,Y., Chen,S.-R. and Liu,Y.-X. (2018) CRISPR/Cas9-mediated genome editing induces gene knockdown by altering the pre-mRNA splicing in mice. *BMC Biotechnol.*, **18**, 61.
11. Mou,H., Smith,J.L., Peng,L., Yin,H., Moore,J., Zhang,X.-O., Song,C.-Q., Sheel,A., Wu,Q., Ozata,D.M., *et al.* (2017) CRISPR/Cas9-mediated genome editing induces exon skipping by alternative splicing or exon deletion. *Genome Biol.*, **18**, 108.
12. Yuan,J., Ma,Y., Huang,T., Chen,Y., Peng,Y., Li,B., Li,J., Zhang,Y., Song,B., Sun,X., *et al.* (2018) Genetic Modulation of RNA Splicing with a CRISPR-Guided Cytidine Deaminase. *Mol. Cell*, **72**, 380-394.e7.
13. Abudayyeh,O.O., Gootenberg,J.S., Konermann,S., Joung,J., Slaymaker,I.M., Cox,D.B.T., Shmakov,S., Makarova,K.S., Semenova,E., Minakhin,L., *et al.* (2016) C2c2 is a single-component programmable RNA-guided RNA-targeting CRISPR effector. *Science*, **353**, aaf5573.
14. East-Seletsky,A., O'Connell,M.R., Knight,S.C., Burstein,D., Cate,J.H.D., Tjian,R. and Doudna,J.A. (2016) Two distinct RNase activities of CRISPR-C2c2 enable guide-RNA processing and RNA detection. *Nature*, **538**, 270–273.
15. Konermann,S., Lotfy,P., Brideau,N.J., Oki,J., Shokhirev,M.N., Hsu,P.D., Effectors,T.V.C., Konermann,S., Lotfy,P., Brideau,N.J., *et al.* (2018) Transcriptome Engineering with RNA-Targeting Type VI-D CRISPR Effectors. *Cell*, **173**, 665-676.e14.
16. Cox,D.B.T., Gootenberg,J.S., Abudayyeh,O.O., Franklin,B., Kellner,M.J., Joung,J. and Zhang,F. (2017) RNA editing with CRISPR-Cas13. *Science (80).*, **358**, 1019–1027.
17. Wessels,H.H., Méndez-Mancilla,A., Guo,X., Legut,M., Daniloski,Z. and Sanjana,N.E. (2020) Massively parallel Cas13 screens reveal principles for guide RNA design. *Nat. Biotechnol.*, **38**, 139–148.
18. Yang,L.-Z.Z., Wang,Y., Li,S.-Q.Q., Yao,R.-W.W., Luan,P.-F.F., Wu,H., Carmichael,G.G. and Chen,L.-L.L. (2019) Dynamic Imaging of RNA in Living Cells by CRISPR-Cas13 Systems. *Mol. Cell*, **76**, 1–17.

19. Siqi Li1, 4, Xiang Li1, 4, Wei Xue2, 4, Lin Zhang1, 4, Shi-Meng Cao1, Yun-Ni Lei2, 3, Liang- Zhong Yang1, Si-Kun Guo1, Jia-Lin Zhang2, Xiang Gao1, 3, Jia Wei2, Jinsong Li1, 3*, Li Yang2, 3,*, Ling-Ling Chen1,3 and 1State (2020) Screening for functional circular RNAs using the CRISPR-Cas13 system. *Bioarxv*.
20. Yang,L.Z., Wang,Y., Li,S.Q., Yao,R.W., Luan,P.F., Wu,H., Carmichael,G.G. and Chen,L.L. (2019) Dynamic Imaging of RNA in Living Cells by CRISPR-Cas13 Systems. *Mol. Cell*, **76**, 981-997.e7.
21. Qu,L., Yi,Z., Zhu,S., Wang,C., Cao,Z., Zhou,Z., Yuan,P., Yu,Y., Tian,F., Liu,Z., *et al.* (2019) Author Correction: Programmable RNA editing by recruiting endogenous ADAR using engineered RNAs. *Nat. Biotechnol.*, **37**, 1380.
22. Wilson,C., Chen,P.J., Miao,Z. and Liu,D.R. (2020) Programmable m6A modification of cellular RNAs with a Cas13-directed methyltransferase. *Nat. Biotechnol.*, **38**, 1431–1440.
23. Leclair,N.K., Brugiolo,M., Urbanski,L., Lawson,S.C., Thakar,K., Yurieva,M., George,J., Hinson,J.T., Cheng,A., Graveley,B.R., *et al.* (2020) Poison Exon Splicing Regulates a Coordinated Network of SR Protein Expression during Differentiation and Tumorigenesis. *Mol. Cell*, **80**, 648-665.e9.
24. Bi,D., Yao,J., Wang,Y., Qin,G., Zhang,Y., Wang,Y. and Zhao,J. (2021) CRISPR/Cas13d-mediated efficient KDM5B mRNA knockdown in porcine somatic cells and parthenogenetic embryos. *Reproduction*, **162**, 149–160.
25. Kushawah,G., Hernandez-Huertas,L., Abugattas-Nuñez del Prado,J., Martinez-Morales,J.R., DeVore,M.L., Hassan,H., Moreno-Sanchez,I., Tomas-Gallardo,L., Diaz-Moscoso,A., Monges,D.E., *et al.* (2020) CRISPR-Cas13d Induces Efficient mRNA Knockdown in Animal Embryos. *Dev. Cell*, 10.1016/j.devcel.2020.07.013.
26. Buchman,A.B., Brogan,D.J., Sun,R., Yang,T., Hsu,P.D. and Akbari,O.S. (2020) Programmable RNA Targeting Using CasRx in Flies. *Cris. J.*, **3**, 164–176.
27. Huynh,N., Depner,N., Larson,R. and King-Jones,K. (2020) A versatile toolkit for CRISPR-Cas13-based RNA manipulation in Drosophila. *Genome Biol.*, **21**, 279.
28. Wang,Q., Liu,Y., Han,C., Yang,M., Huang,F., Duan,X., Wang,S., Yu,Y., Liu,J., Yang,H., *et al.* (2021) Efficient RNA Virus Targeting via CRISPR/CasRx in Fish. *J. Virol.*, **95**, e0046121.
29. Mahas,A., Aman,R. and Mahfouz,M. (2019) CRISPR-Cas13d mediates robust RNA virus interference in plants. *Genome Biol.*, **20**, 1–16.
30. Zhang,K., Zhang,Z., Kang,J., Chen,J., Liu,J., Gao,N., Fan,L., Zheng,P., Wang,Y. and Sun,J. (2020) CRISPR/Cas13d-Mediated Microbial RNA Knockdown. *Front. Bioeng. Biotechnol.*, **8**, 1–9.
31. Meeske,A.J., Nakandakari-Higa,S. and Marraffini,L.A. (2019) Cas13-induced cellular dormancy prevents the rise of CRISPR-resistant bacteriophage. *Nature*, **570**, 241–245.
32. Yanagisawa,M., Huveldt,D., Kreinest,P., Lohse,C.M., Cheville,J.C., Parker,A.S., Copland,J.A. and Anastasiadis,P.Z. (2008) A p120 catenin isoform switch affects rho activity, induces tumor cell invasion, and predicts metastatic disease. *J. Biol. Chem.*, **283**, 18344–18354.
33. Segelle,A., Núñez-Álvarez,Y., Oldfield,A.J., Webb,K.M., Voigt,P. and Luco,R.F. (2021) Histone marks are drivers of the splicing changes necessary for an epithelial-to-mesenchymal transition. *bioRxiv*, 10.1101/2021.05.04.442453.
34. Labun,K., Montague,T.G., Krause,M., Torres Cleuren,Y.N., Tjeldnes,H. and Valen,E.

(2019) CHOPCHOP v3: expanding the CRISPR web toolbox beyond genome editing. *Nucleic Acids Res.*, **47**, W171–W174.

35. Tang,S.J., Luo,S., Ho,J.X.J., Ly,P.T., Goh,E. and Roca,X. (2016) Characterization of the regulation of CD46 RNA alternative splicing. *J. Biol. Chem.*, **291**, 14311–14323.
36. Ule,J. and Blencowe,B.J. (2019) Alternative Splicing Regulatory Networks: Functions, Mechanisms, and Evolution. *Mol. Cell*, **76**, 329–345.
37. Luo,W. and Semenza,G.L. (2012) Emerging roles of PKM2 in cell metabolism and cancer progression. *Trends Endocrinol. Metab.*, **23**, 560–566.
38. Piva,F., Giulietti,M., Burini,A.B. and Principato,G. (2012) SpliceAid 2: a database of human splicing factors expression data and RNA target motifs. *Hum. Mutat.*, **33**, 81–85.
39. Wang,Z., Jeon,H.Y., Rigo,F., Bennett,C.F, Krainer,A.R. (2012) Manipulation of PK-M mutually exclusive alternative splicing by antisense oligonucleotides. *Open Biol.*, **2(10)**, 120133.
40. Wang,Z., Chatterjee,D., Jeon,H.Y., Akerman,M., Vander Heiden,M.G., Cantley,L.C. and Krainer,A.R. (2012) Exon-centric regulation of pyruvate kinase M alternative splicing via mutually exclusive exons. *J. Mol. Cell Biol.*, **4**, 79–87.
41. Kuranaga,Y., Sugito,N., Shinohara,H., Tsujino,T., Taniguchi,K., Komura,K., Ito,Y., Soga,T. and Akao,Y. (2018) SRSF3, a splicer of the PKM gene, regulates cell growth and maintenance of cancer-specific energy metabolism in colon cancer cells. *Int. J. Mol. Sci.*, **19**, 1–16.
42. Koren,E., Lev-Maor,G. and Ast,G. (2007) The emergence of alternative 3′ and 5′ splice site exons from constitutive exons. *PLoS Comput. Biol.*, **3**, 0895–0908.
43. Bielli,P., Bordi,M., Di Biasio,V. and Sette,C. (2014) Regulation of BCL-X splicing reveals a role for the polypyrimidine tract binding protein (PTBP1/hnRNP I) in alternative 5′ splice site selection. *Nucleic Acids Res.*, **42**, 12070–12081.

FIGURE LEGENDS

Figure 1. Position-dependent effect of dCasRx-mediated modulation of splicing.

Figure 2. dCasRx is an efficient tool to edit splicing.

Figure 3. dCasRx position-dependent effect underlines the existence of key cis-regulatory RNA elements at the targeted exon.

Figure 4. dCasRx can be used to identify unsuspected regulatory mechanisms.

Figure 5. Position-specific targeting of dCasRx helps identifying key splicing regulators**.**

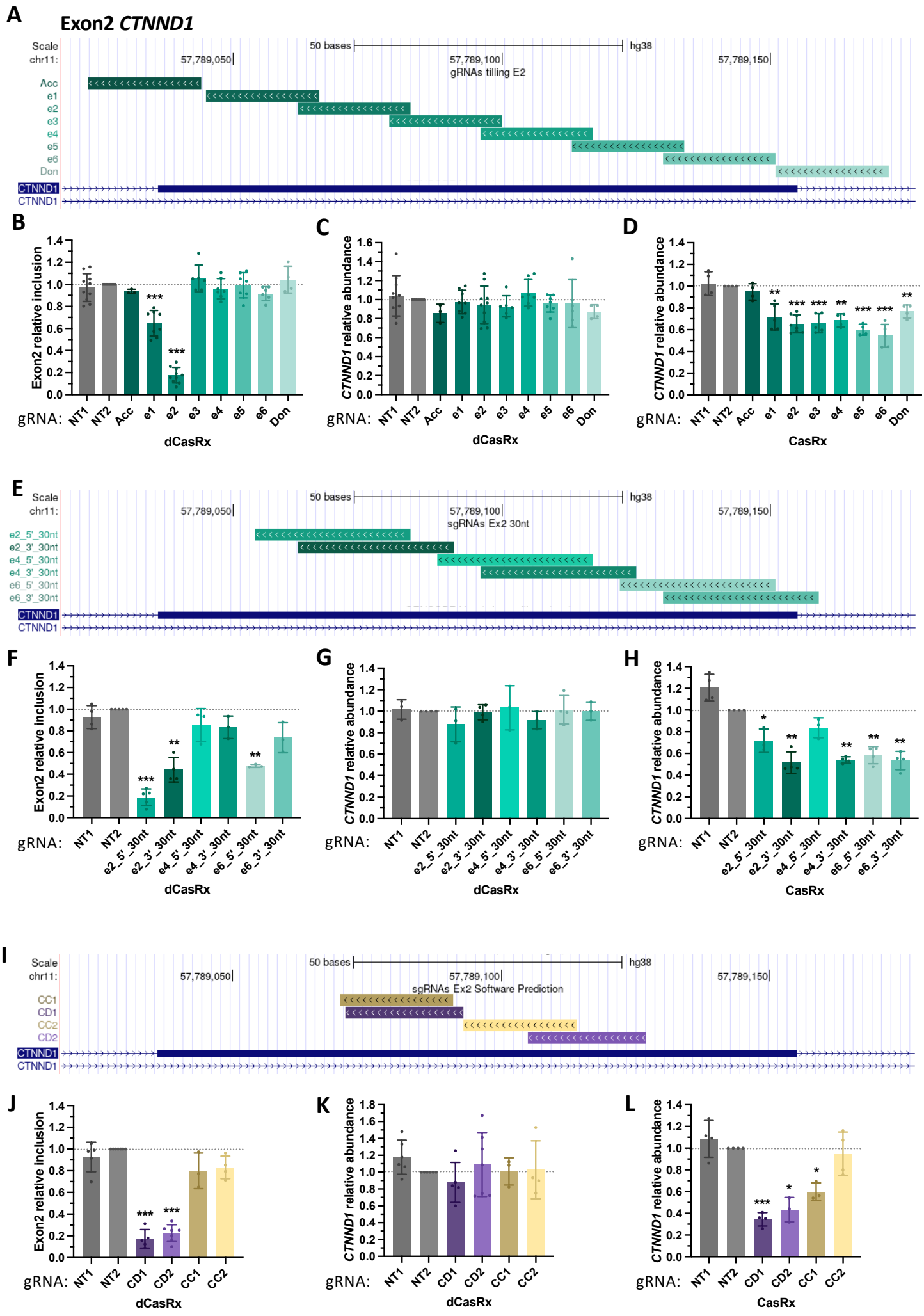

Figure 1. Position-dependent effect of dCasRx-mediated modulation of splicing. (**A**) Genome positioning along *CTNND1* exon 2 of a tilling array of 8 overlapping gRNAs going from the acceptor (Acc) splice site to the donor (Don) site. (**B**) *CTNND1* exon 2 relative inclusion levels in HEK293T cells after 72h transfection with 200ng of dCasRx and 200ng of the indicated gRNA. RT-qPCR levels are normalized by total gene expression levels and represented as mean respect Non-Targeting gRNA 2 (NT2) levels. (**C,D**) *CTNND1* relative abundance levels in HEK293T cells after 72h transfection with 200ng of dCasRx (C) or CasRx (D) and 200ng of the indicated gRNA. RT-qPCR levels are normalized by *TBP* and Non-Targeting gRNA gRNA 2 (NT2). (**E**) Genome positioning along *CTNND1* exon 2 of the 5´ or 3´ extended gRNAs corresponding to gRNA.e2, e4 and e6. (**F**) *CTNND1* exon 2 relative inclusion levels in HEK293T cells after 72h transfection with 200ng of dCasRx and 200ng of the indicated 30nt-extended gRNA. RT-qPCR levels are normalized by total gene expression levels and represented as mean respect Non-Targeting gRNA 2 (NT2) levels. (**G, H**) CTNND1 relative abundance levels in HEK293T cells after 72h transfection with 200ng of dCasRx (G) or CasRx (H) and 200ng of the indicated gRNA. RT-qPCR levels are normalized by *TBP* and non targeting gRNA 2 (NT2). (**I**) Genome positioning of the best ranked gRNAs of *CTNND1* exon 2 using "Cas13design" (CD, purple shades) and CHOPCHOP (CC, yellow shades) web tools. (**J**) *CTNND1* exon 2 relative inclusion levels in HEK293T cells after 72h transfection with 200ng of dCasRx and 200ng of the indicated gRNA. RT-qPCR levels are normalized by total gene expression levels and represented as mean respect Non-Targeting gRNA 2 (NT2) levels. (**K, L**) CTNND1 relative abundance levels in HEK293T cells after 72h transfection with 200ng of dCasRx (K) or CasRx (L) and 200ng of the indicated gRNA. RT-qPCR levels are normalized by *TBP* and non targeting gRNA 2 (NT2). Data correspond in all cases to the average of at least 3 biological independent experiments ± SD. **P* <0.05, ***P* <0.01, ****P* <0.001 in two-tail not paired Student's t-test respect NT1 and NT2 gRNAs independently (grey).

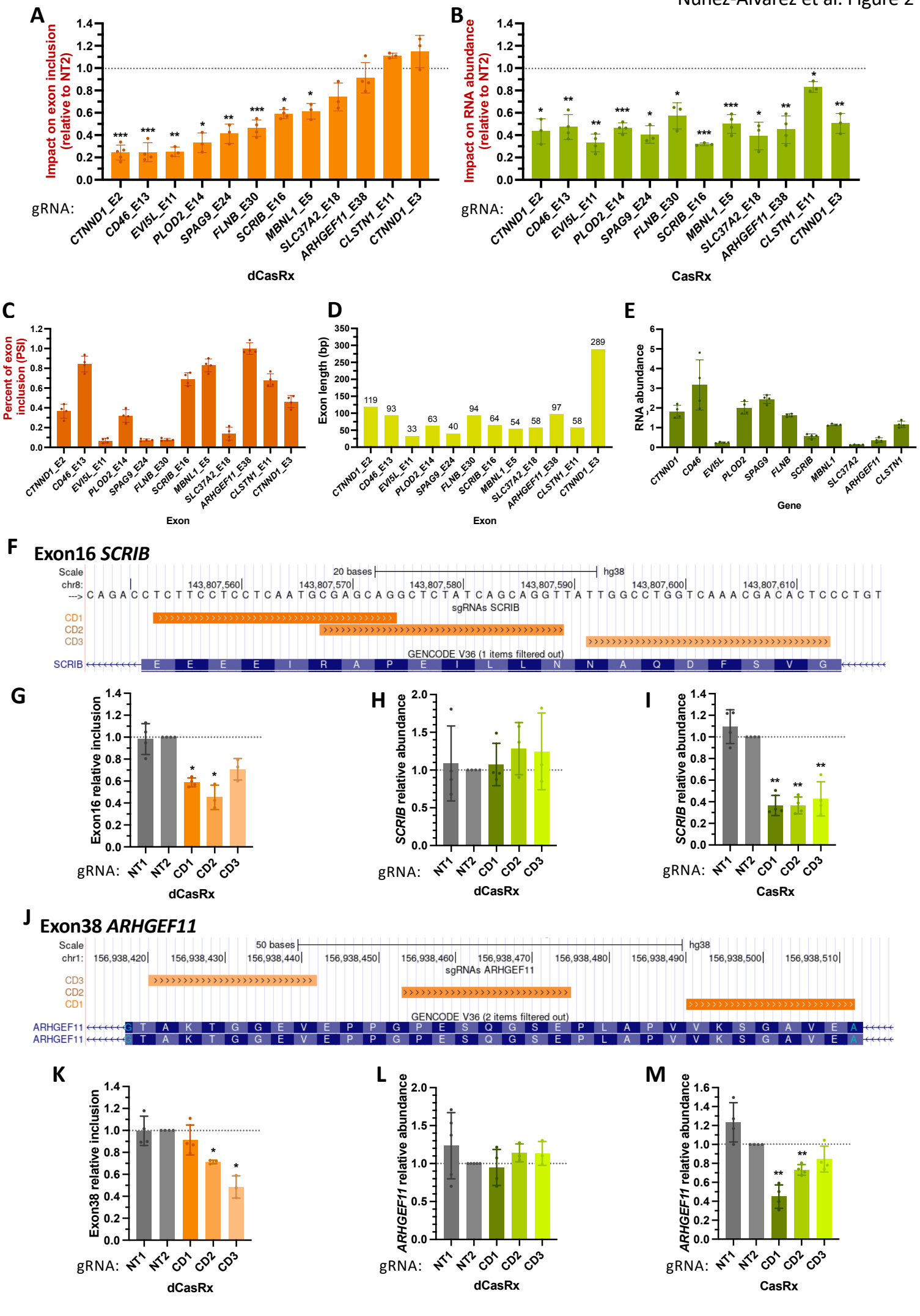

Figure 2. dCasRx is an efficient tool to edit splicing. (**A**) Impact on the inclusion levels of 12 alternatively spliced exons upon transfection in HEK293T cells of dCasRx and the top scored gRNAs targeting each exon using the "cas13design" web tool (https://cas13design.nygenome.org/). RT-qPCR levels were normalized by total expression levels of the corresponding gene and represented as mean +/- SD of at least 3 biological replicates respect Non-Targeting gRNA 2 (NT2). (**B**) Impact on RNA abundance at the genes targeted with the gRNAs described in (A) and CasRx. RT-qPCR levels were normalized by *TBP* and represented as mean +/- SD of at least 3 biological replicates respect Non-Targeting gRNA 2 (NT2). (**C**) Percent of exon inclusion (known ad PSI) of the 12 alternatively spliced exons studied in (A) in non-edited HEK293T cells. RT-qPCR levels were normalized to total gene expression levels of the corresponding gene in n=4 biological replicates. (**D**) Exon size in nucleotides (bp) of the 12 alternatively spliced exons studied in (A). (**E**) Gene expression levels of the 12 alternatively spliced genes studied in (A) before targeting. RT-qPCR levels were normalized to *TBP* and represented as mean +/- SD of n=4 biological replicates. (**F)** Genomic positioning along *SCRIB* exon 16 of the three non-overlapping top scored gRNAs predicted by the "cas13design" tool. (**G**) *SCRIB* Exon 16 inclusion levels in HEK293T cells after 72h transfection with 200ng of dCasRx and 200ng of the indicated gRNA. RT-qPCR levels were normalized by total gene expression levels and represented as mean +/- SD of at least 3 biological replicates respect Non-Targeting gRNA 2 (NT2) levels. (**H, I**) *SCRIB* relative gene abundance upon transfection with 200ng of gRNA and 200 ng of dCasRx (H) or CasRx (I) in HEK293 cells. RT-qPCR levels are normalized by TBP and non targeting gRNA 2 (NT2) in at least biological replicates". (**J**) *ARHGEF11* Exon 38 inclusion levels in HEK293T cells after 72h transfection with 200ng of dCasRx and 200ng of the indicated gRNA. RT-qPCR levels were normalized by total gene expression levels and represented as mean +/- SD of at least 3 biological replicates respect Non-Targeting gRNA 2 (NT2) levels. (**K, L**) *ARHGEF11* relative gene abundance level upon transfection with 200ng of gRNA and 200 ng of dCasRx (L) or CasRx (M) in HEK293T cells. RT-qPCR levels were normalized by *TBP* and non targeting gRNA 2 (NT2) in at least 3 biological replicates. **P* <0.05, ***P* <0.01, ****P* <0.001 in two-tail not paired Student's t-test respect NT1 and NT2 gRNAs independently (grey).

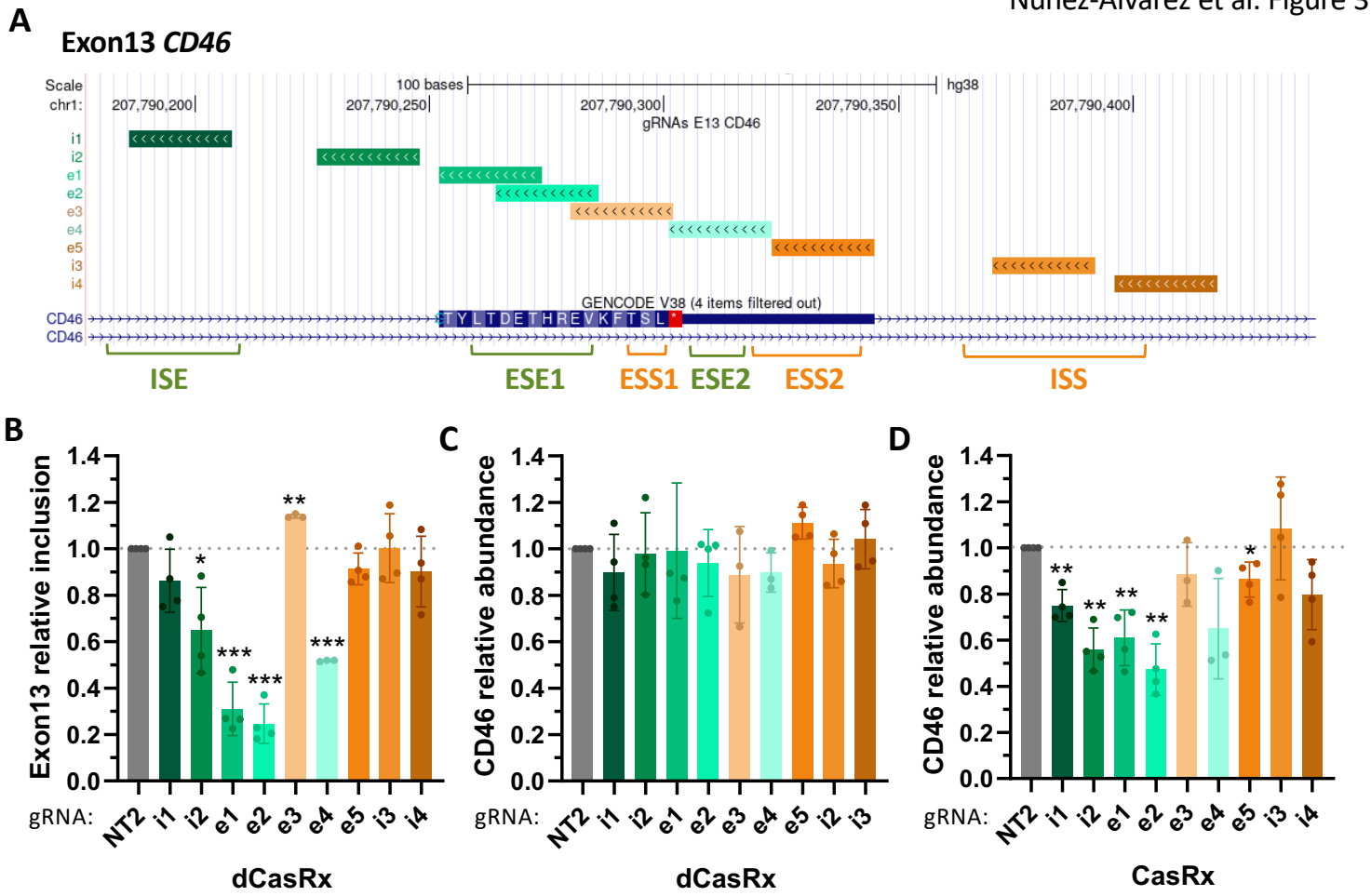

Figure 3. dCasRx position-dependent effect underlines the existence of key cis-regulatory elements at the targeted exon. (**A**) Genomic positioning along *CD46* exon 14 and flanking introns of gRNAs targeting well-defined exonic (e1-e4) and intronic (i1-i4) regulatory regions. In green are represented the splicing enhancers and in orange the splicing silencers according to Tang et al., 2016 J. Biol. Chem (Ref. 35). (**B**) *CD46* exon 13 relative inclusion levels in HEK293T cells after 72h transfection with 200ng of dCasRx and 200ng of the indicated gRNA. RT-qPCR levels were normalized by total gene expression levels and represented as mean +/- SD of n=4 biological replicates respect Non-Targeting gRNA 2 (NT2) levels. (**C, D**) *CD46* relative gene abundance levels upon transfection with 200ng of gRNA and 200 ng of dCasRx (C) or CasRx (D) in HEK293T cells. RT-qPCR levels were normalized by *TBP* and non targeting gRNA 2 (NT2) in n=4 biological replicates. **P* <0.05, ***P* <0.01, ****P* <0.001 in two-tail not paired Student's t-test respect NT1 and NT2 gRNAs independently (grey).

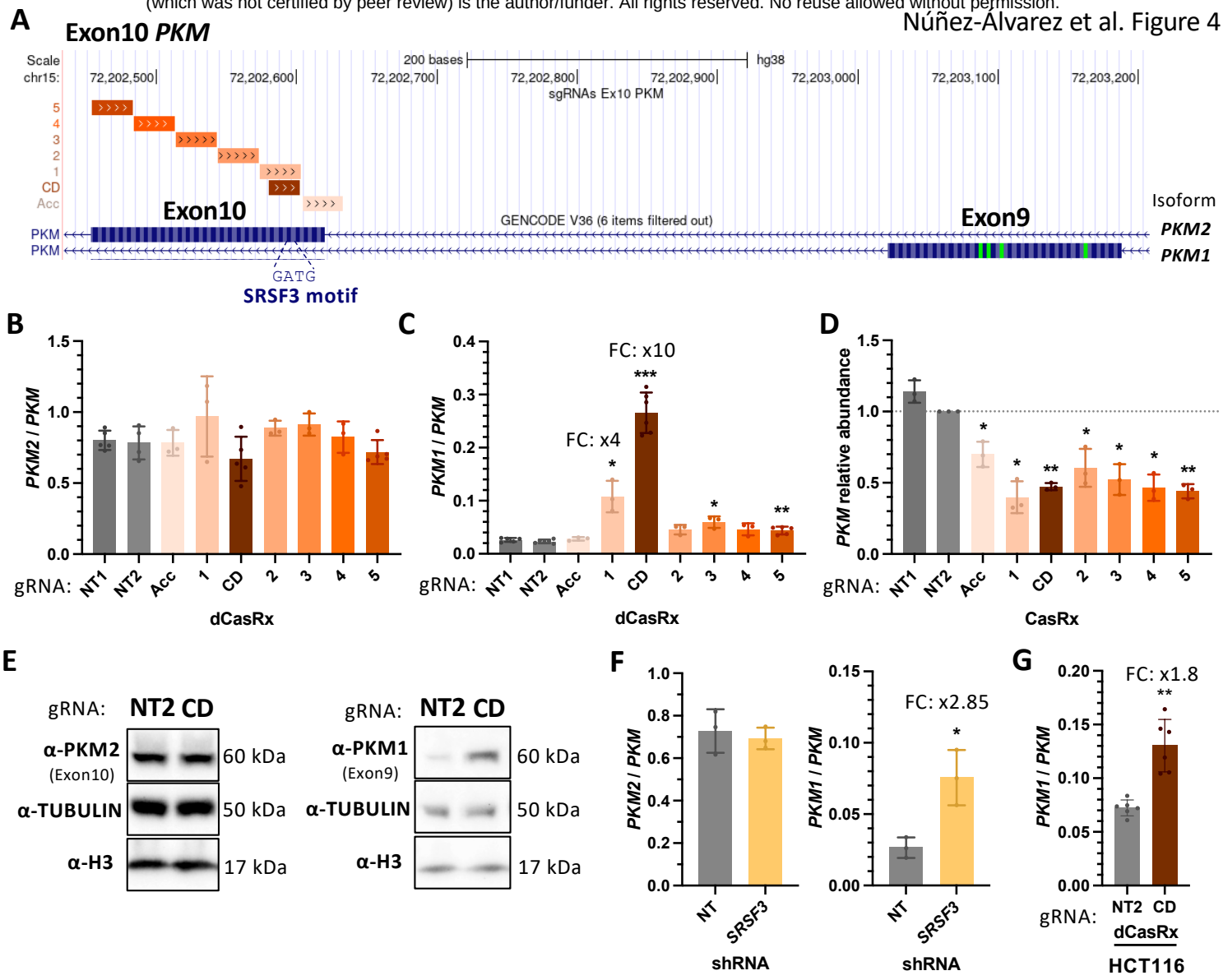

Figure 4. dCasRx splicing editing can be used to identify key regulatory mechanisms. (**A**) Genomic positioning of a tilling array of home-made gRNAs spanning *PKM* exon 10. The top scored gRNA predicted with "Cas13design" is shown in brown (CD). *PKM* is alternatively spliced into two mutually exclusive isoforms: *PKM1* that includes exon 9 and *PKM2* that includes exon 10. HEK293T cells express mostly the *PKM2* isoform. SRSF3 motif (GATG) was found at *PKM* exon 10 with the top score using SpliceAid RNA motif database (http://www.introni.it/splicing.html). (**B,C**) *PKM2* isoform (exon 10, B) and *PKM1* isoform (exon 9, C) inclusion levels in HEK293T cells after 72h transfection with 200ng of dCasRx and 200ng of the indicated gRNA. RT-qPCR levels are normalized by total gene expression levels and represented as mean +/- SD. (**D**) *PKM* relative abundance levels in HEK293T cells after 72h transfection with 200ng of CasRx and 200ng of the indicated gRNA. RT-qPCR levels are normalized by *TBP* and non targeting gRNA 2 (NT2) and represented as mean +/- SD of at least 3 biological replicates. (**E**) Representative western blot images detecting PKM2 and PKM1 PKM isoforms and TUBULIN and H3 proteins as loading controls in HEK293T cells transfected with dCasRx and the best editing gRNA (CD). Non targeting gRNA NT2 was used as a negative control. (**F**) Impact of shRNA-mediated *SRSF3* knock-down in *PKM* exon 10 and exon 9 inclusion levels in HEK293T cells. RT-qPCR levels are normalized by total gene expression levels and represented as mean +/- SD of n=3 biological replicates. A non-targeting shRNA was used as control (NT). (**G**) *PKM* exon 9 inclusion levels in HCT116 cells after 72h transfection with 200ng of dCasRx and 200ng of gRNA CD. RT-qPCR levels are normalized by total gene expression levels and represented as mean +/- SD of n=6 biological replicates. *P <0.05, **P <0.01, ***P <0.001, in two-tail not paired Student's t-test respect NT1 and NT2 gRNAs independently (grey).

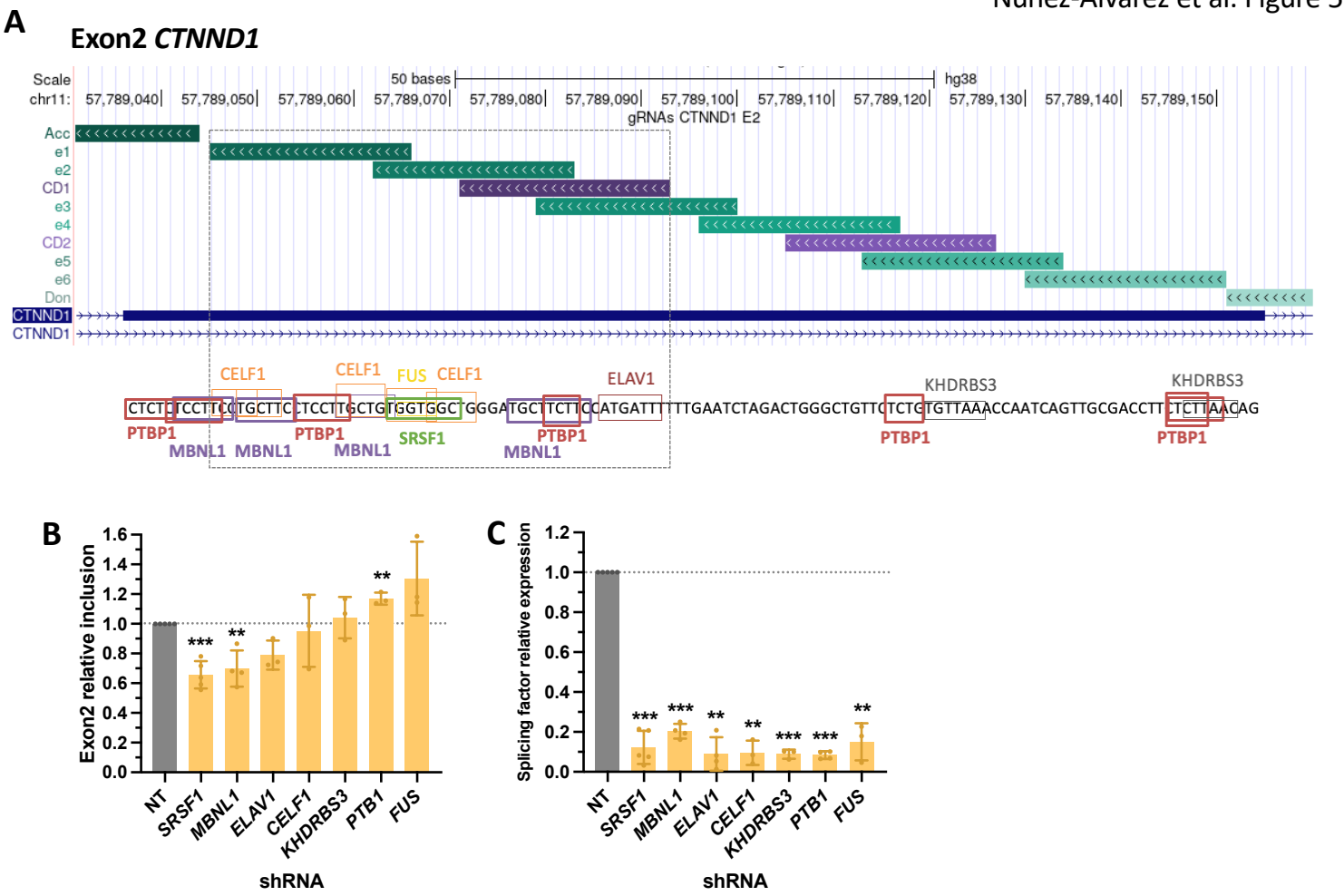

Figure 5. dCasRx can be used to identify regulatory mechanisms of splicing. (**A**) RNA binding motifs along *CTNND1* exon 2 pre-mRNA predicted by at least two of the four publicly available RNA motif databases used (RBPDB, RBPMAP, SFMAP and Spliceaid). The genomic position of the gRNAs most impacting *CTNND1* splicing are also shown in a dotted square. (**B**) *CTNND1* exon 2 relative inclusion levels in HEK293T cells upon shRNA-mediated knock-down of the splicing factors which motifs are found in (A). RT-qPCR levels are normalized by *TBP* and represented as mean +/-SD relative to non-targeting control shRNA in n=4 biological replicates. (**C**) Knock-down efficiencies of the shRNA tested in (B). RT-qPCR levels are normalized by *TBP* and represented as the mean +/- SD relative to NT shRNA in at least 3 biological replicates. **P* <0.05, ***P* <0.01, ****P* <0.001, in two-tail not paired Student's t-test respect non targeting shRNA (NT, grey).

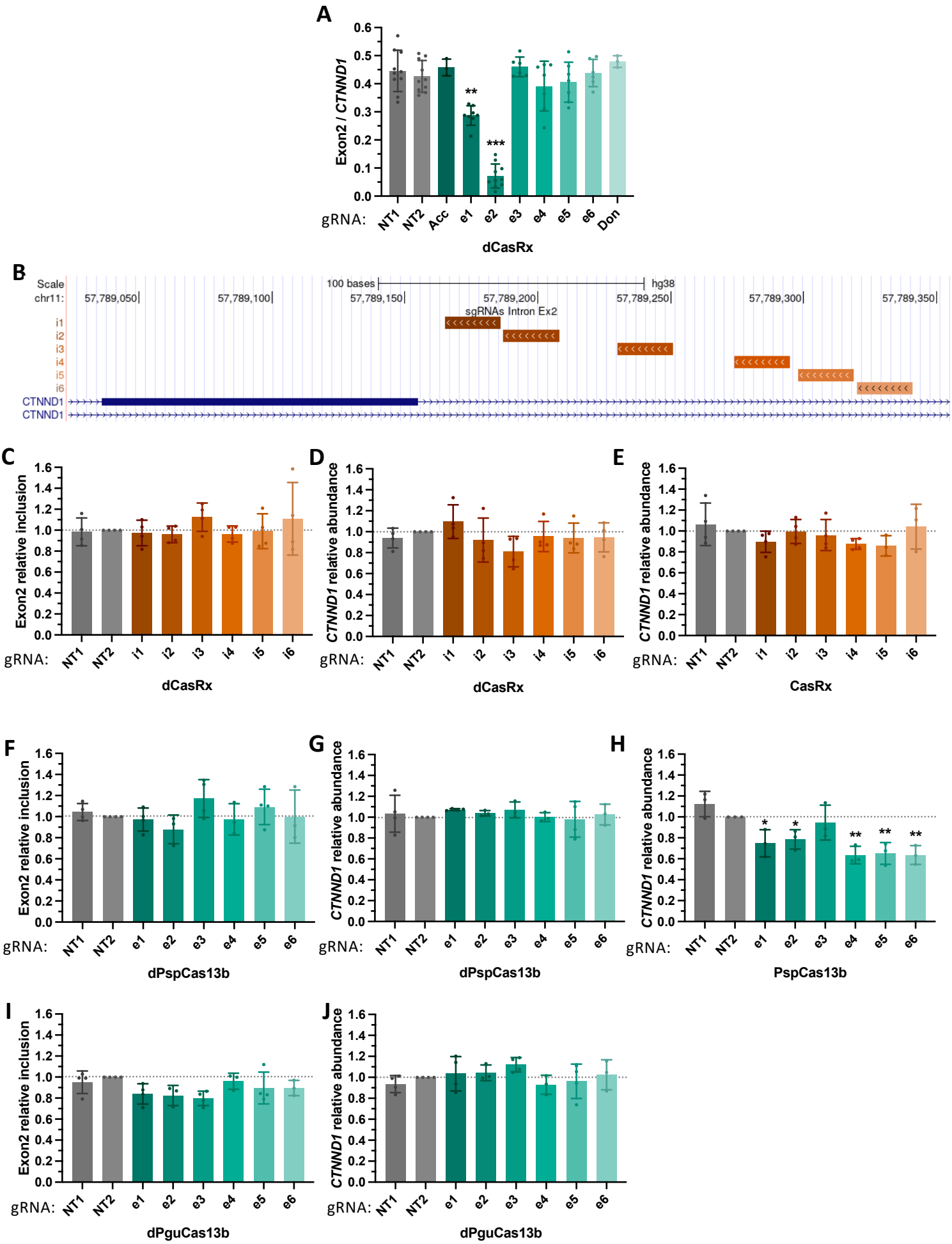

Supplementary Figure 1. Intronic gRNAs and dCas13 from other species do not impact splicing. (**A**) *CTNND1* exon 2 inclusion levels in HEK293T cells after 72h transfection with 200ng of dCasRx and 200ng of the indicated gRNA. RT-qPCR levels are normalized by total gene expression levels and represented as mean +/- SD. (**B**) Genome positioning of gRNAs targeting the downstream intronic region flanking *CTNND1* exon2. (**C**) *CTNND1* exon 2 relative inclusion levels in HEK293T cells after 72h transfection with 200ng of dCasRx and 200ng of the indicated gRNA. RT-qPCR levels are normalized by total gene expression levels and represented as mean +/- SD respect Non-Targeting gRNA 2 (NT2) levels. (**D,E**) *CTNND1* relative abundance in HEK293T cells after 72h transfection with 200ng of dCasRx (D) or CasRx (E) and 200ng of the indicated gRNA. RT-qPCR levels are normalized by *TBP* and non targeting gRNA 2 (NT2). (**F, I**) *CTNND1* exon 2 relative inclusion levels in HEK293T cells after 72h transfection with 200ng of dPspCas13b (F) or dPguCas13b (I) and 200ng of the indicated gRNA. RT-qPCR levels are normalized by total gene expression levels and represented as mean respect Non-Targeting gRNA 2 (NT2) levels. (**G, H, J**) *CTNND1* relative abundance in HEK293T cells after 72h transfection with 200ng of catalytically inactive dPspCas13b (G), dPguCas13b (J) or catalytically active PspCas13b (H) and 200ng of the indicated gRNA. RT-qPCR levels are normalized by *TBP* and non targeting gRNA 2 (NT2). Data correspond in all cases to the average of at least 3 biological independent experiments ± SD. **P* <0.05, ***P* <0.01, ****P* <0.001 in two-tail not paired Student's t-test respect NT1 and NT2 gRNAs independently (grey).

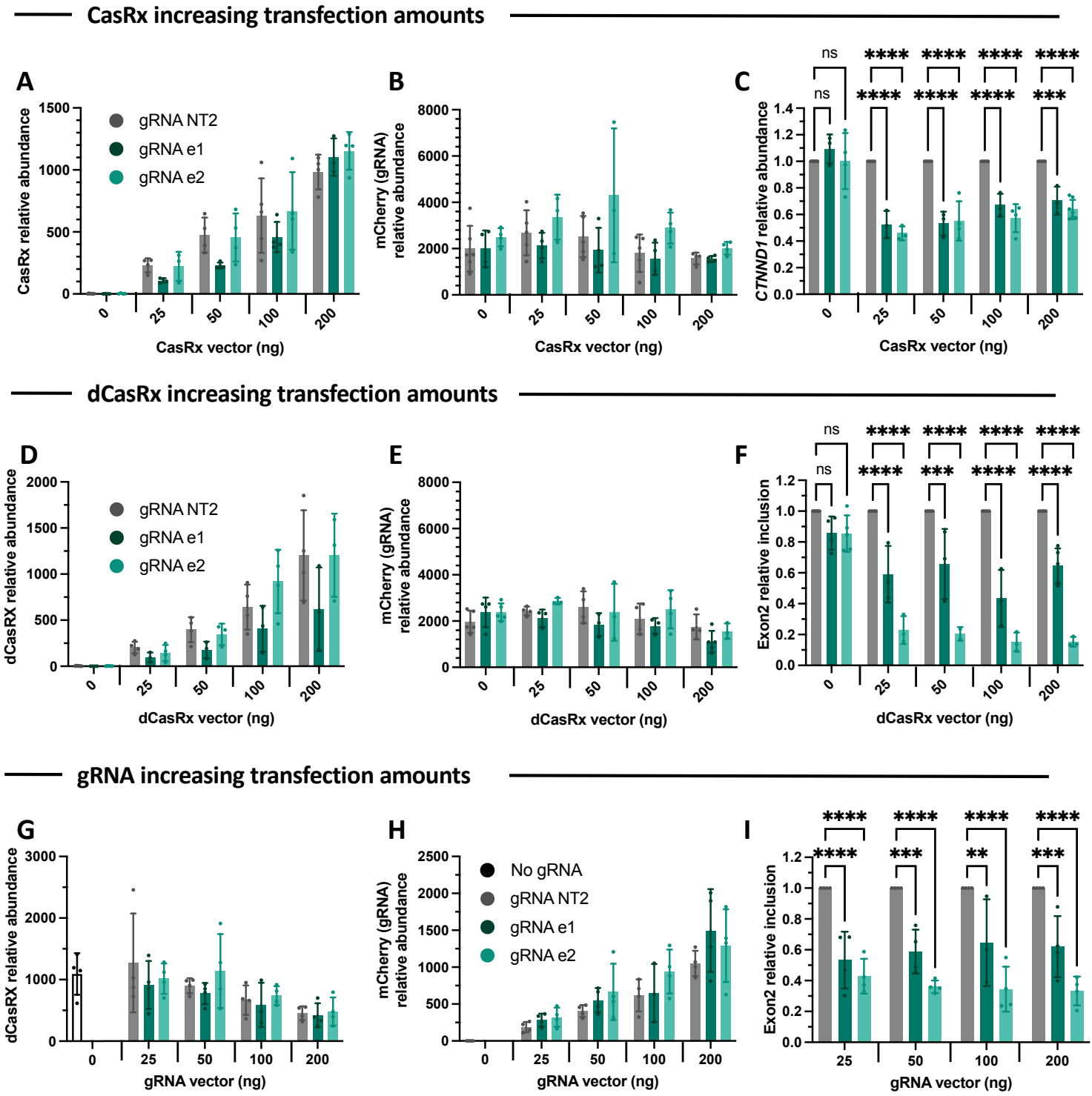

Supplementary Figure 2. CasRx, dCasRx and gRNA levels for RNA knock-down and splicing editing. (**A-C**) HEK293T cells were transfected using Lipofectamine 2000 with 200ng of the indicated gRNAs and increasing amounts of CasRx as indicated (0-200ng). After 72 h, cells were collected and analysed using RT-qPCR for CasRx expression (A), mCherry (co-expressed in gRNA vector, B) and *CTNND1* (C). (**D-F**) HEK293T cells were transfected using Lipofectamine 2000 with 200ng of the indicated gRNAs and increasing amounts of dCasRx as indicated (0-200ng). After 72 h, cells were collected and analysed using RT-qPCR for CasRx expression (D), mCherry (co-expressed in gRNA vector, E) and Exon2 (F). (**G-I**) HEK293T cells were transfected using Lipofectamine2000 with 200ng of dCasRx and increasing amounts of the indicated gRNAs as shown (0-200ng). After 72 h, cells were collected and analysed using RT-qPCR for dCasRx expression (G), mCherry (co-expressed in gRNA vector, H) and Exon2 (I). For all conditions, CasRx/dCasRx, mCherry and *CTNND1* levels were normalized by *TBP* and Exon2 inclusion levels were normalized by *CTNND1* total expression. RT-qPCR levels are shown as the mean +/- SD of at least 3 biologically independent experiments . **P* <0.05, ***P* <0.01, ****P* <0.001, **** *P* <0.0001, in two-way Anova respect NT2 gRNA (grey).

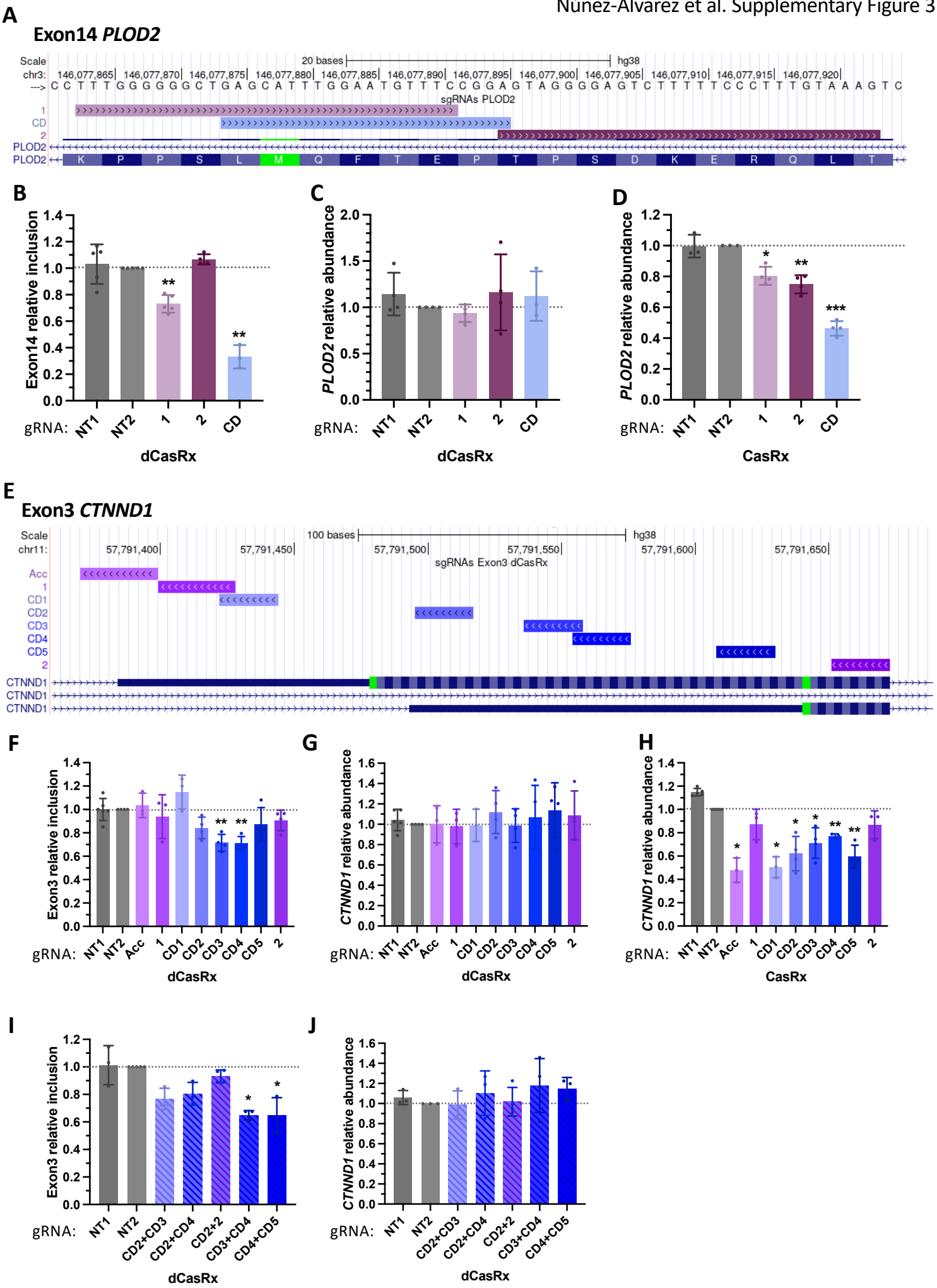

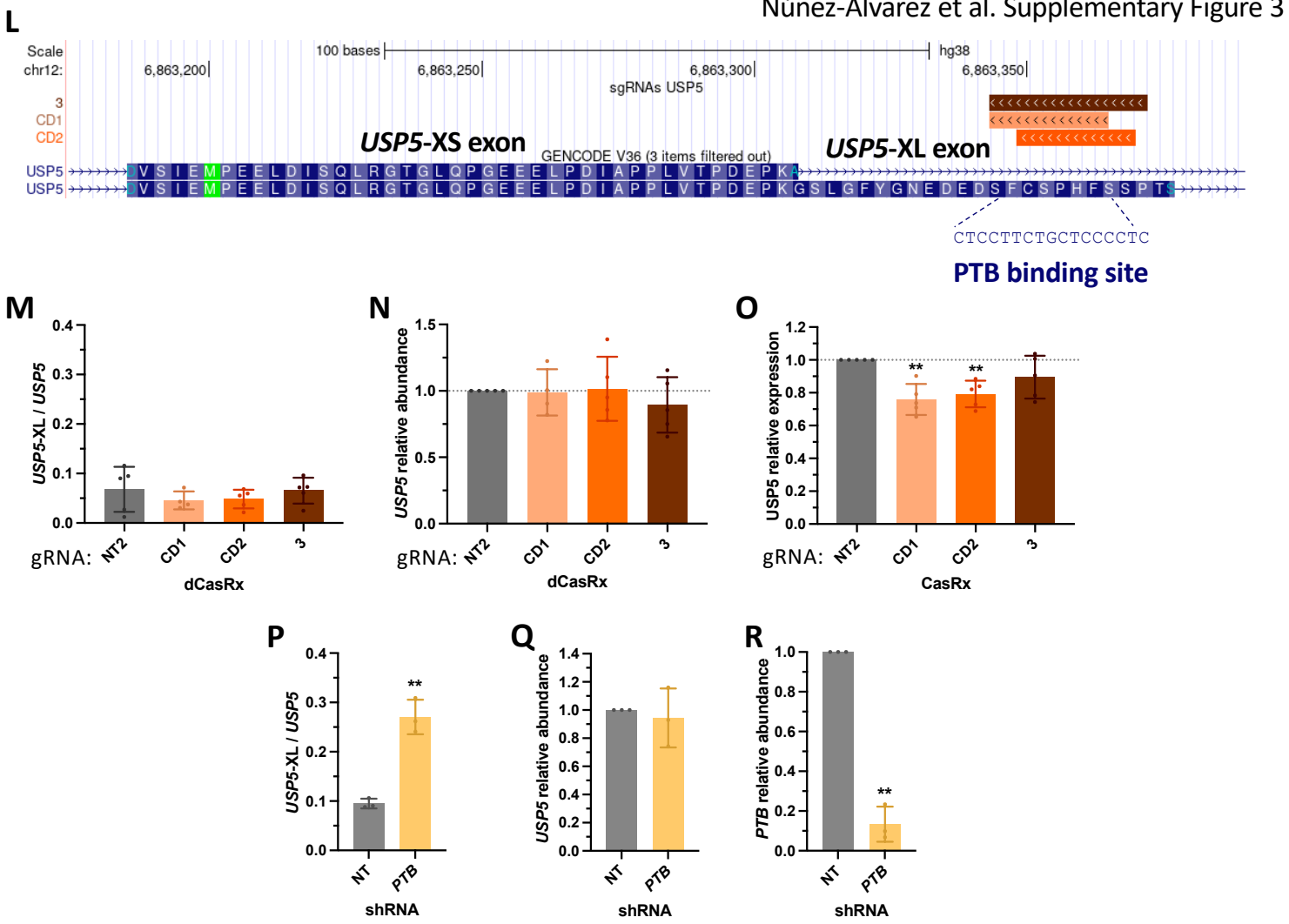

Supplementary Figure 3. gRNAs designed with "Cas13design" edit efficiently splicing. (**A**) Genomic positioning along *PLOD2* exon 14 of two home-made gRNAs and the top scored "Cas13design" gRNA (CD). (**B**) *PLOD2* exon 14 relative inclusion levels in HEK293T cells after 72h transfection with 200ng of dCasRx and 200ng of the indicated gRNA. RT-qPCR levels were normalized by total gene expression levels and represented as mean +/- SD of at least 3 biological replicates respect Non-Targeting gRNA 2 (NT2) levels. (**C, D**) *PLOD2* relative gene abundance levels upon transfection with 200ng of gRNA and 200 ng of dCasRx (C) or CasRx (D) in HEK293T cells. RT-qPCR levels were normalized by *TBP* and non targeting gRNA 2 (NT2). (**E**) Genomic positioning along *CTNND1* exon 3 of top score gRNAs using "Cas13design" tool (CD, blue shades) and home-made (violet shades). (**F,I**) *CTNND1* Exon3 relative inclusion levels in HEK293T cells after 72h transfection with 200ng of dCasRx and 200ng of the indicated gRNAs alone (F) or in combination (I). RT-qPCR levels were normalized by total gene expression levels and represented as mean +/- SD respect Non-Targeting gRNA 2 (NT2) levels. (**G,H,J**) *CTNND1* relative abundance levels upon transfection with 200ng of gRNA and 200 ng of dCasRx (G,J) or CasRx (H) in HEK293T cells. RT-qPCR levels were normalized by *TBP* and non targeting gRNA 2 (NT2). (**L**) Genomic positioning of 3 gRNAs targeting a PTB binding site described by Bielli et al., 2014 to repress USP5-XL splice variant. (**M**) Relative inclusion levels of *USP5* long isoform (XL) in HEK293T cells after 72h transfection with 200ng of dCasRx and 200ng of the indicated gRNA. RT-qPCR levels were normalized by total gene expression levels and represented as mean +/- SD. (**N,O**) *USP5* relative gene abundance levels upon transfection with 200ng of gRNA and 200 ng of dCasRx (M) or CasRx (N) in HEK293T cells. RT-qPCR levels were normalized by TBP in at least 4 biological replicates. (**P**) Effect of shRNA-mediated *PTB* knock-down in *USP5*-XL splicing. As described, in the absence of PTB there is a change in the 5' splice site used with an increase in expression levels of the long isoform respect the short. RT-qPCR levels were normalized to total gene expression levels in n=3 biological replicates. (**Q**) *USP5* total levels after *PTB* knco-down. (**R**) *PTB* knock-down efficiency using shRNA in HEK293T cells. *PTB* RT-qPCR levels were normalized to *TBP* in n=3 biological replicates. **P* <0.05, ***P* <0.01, ****P* <0.001, in two-tail not paired Student's t-test respect NT2 gRNAs (grey).

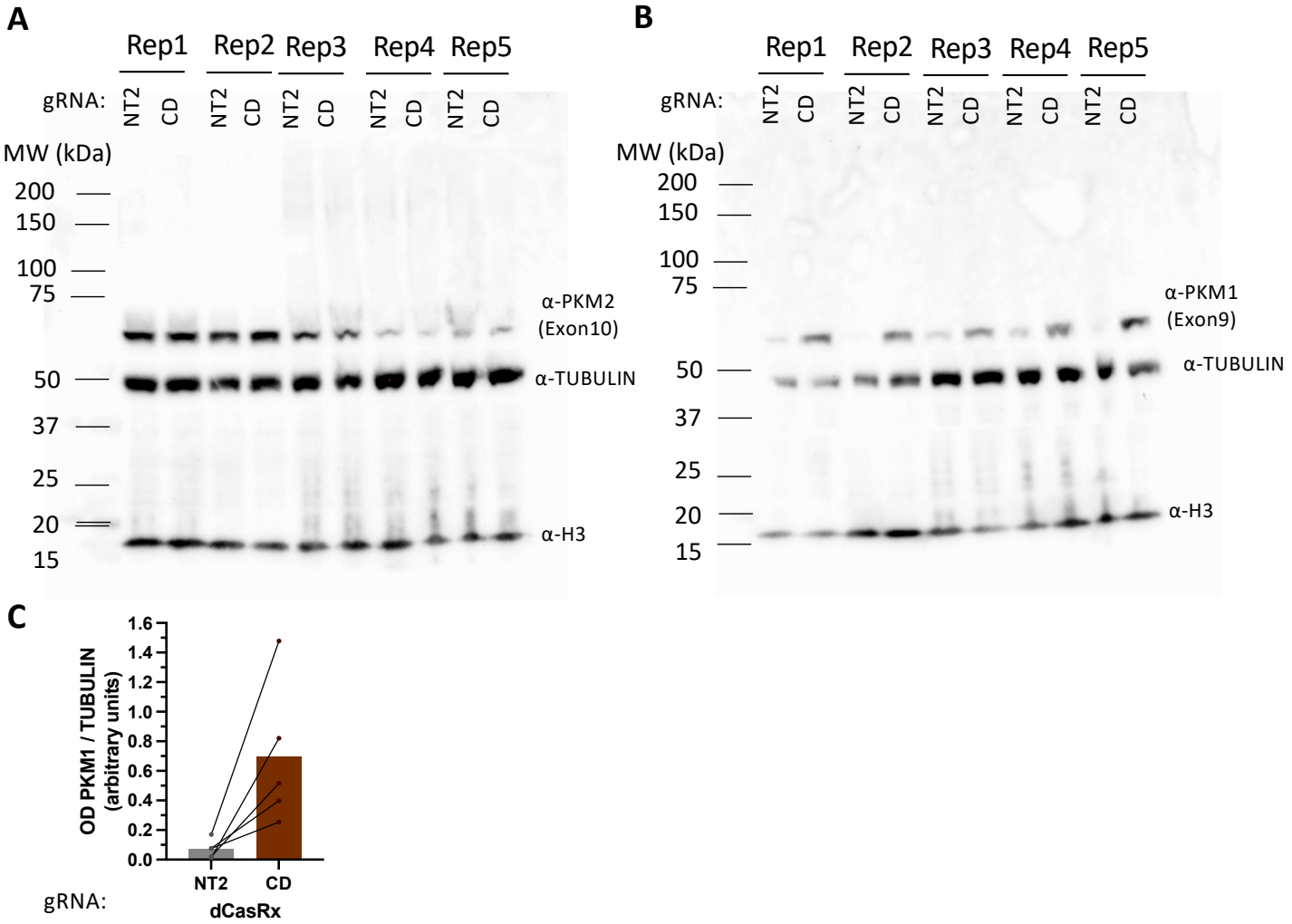

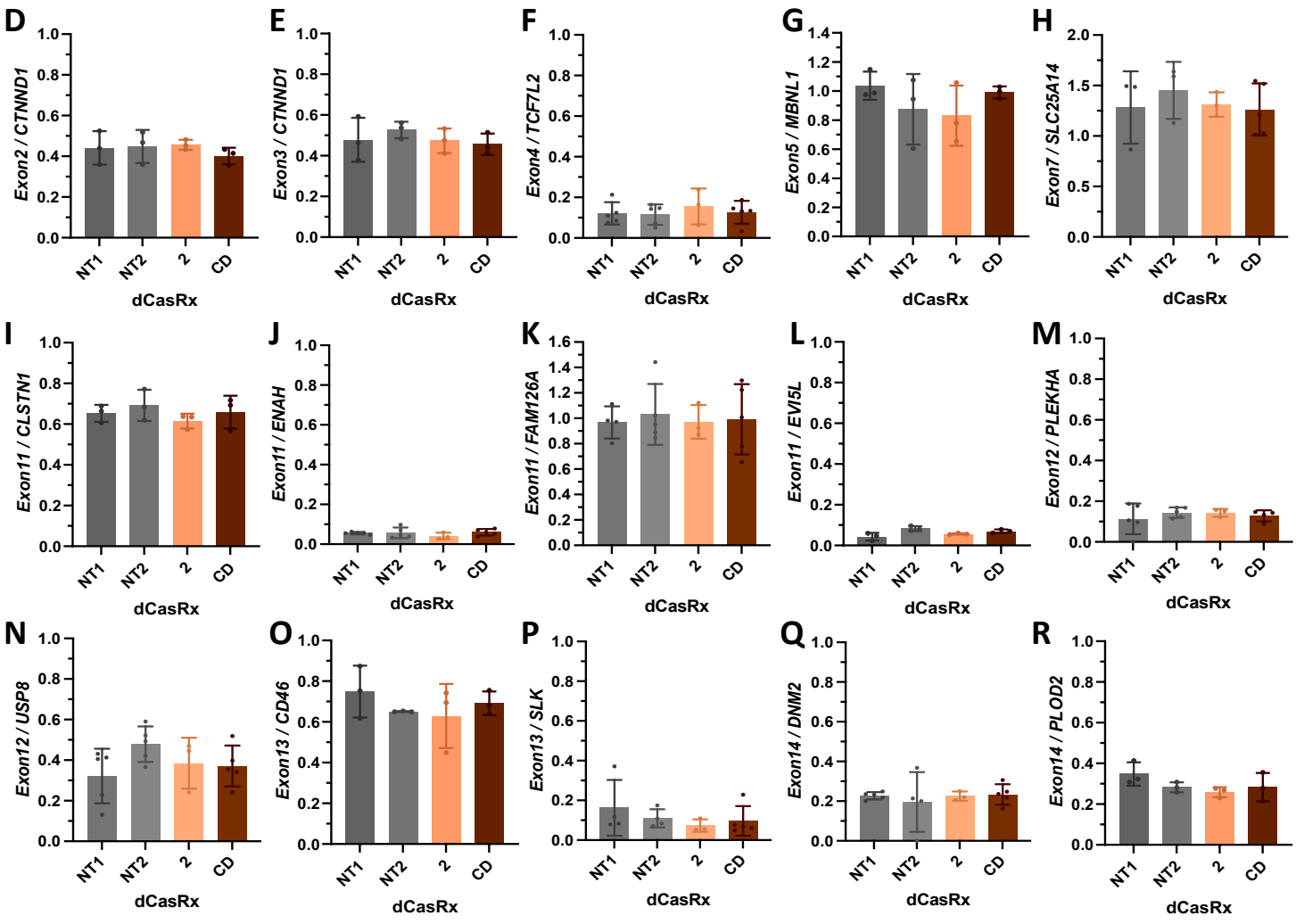

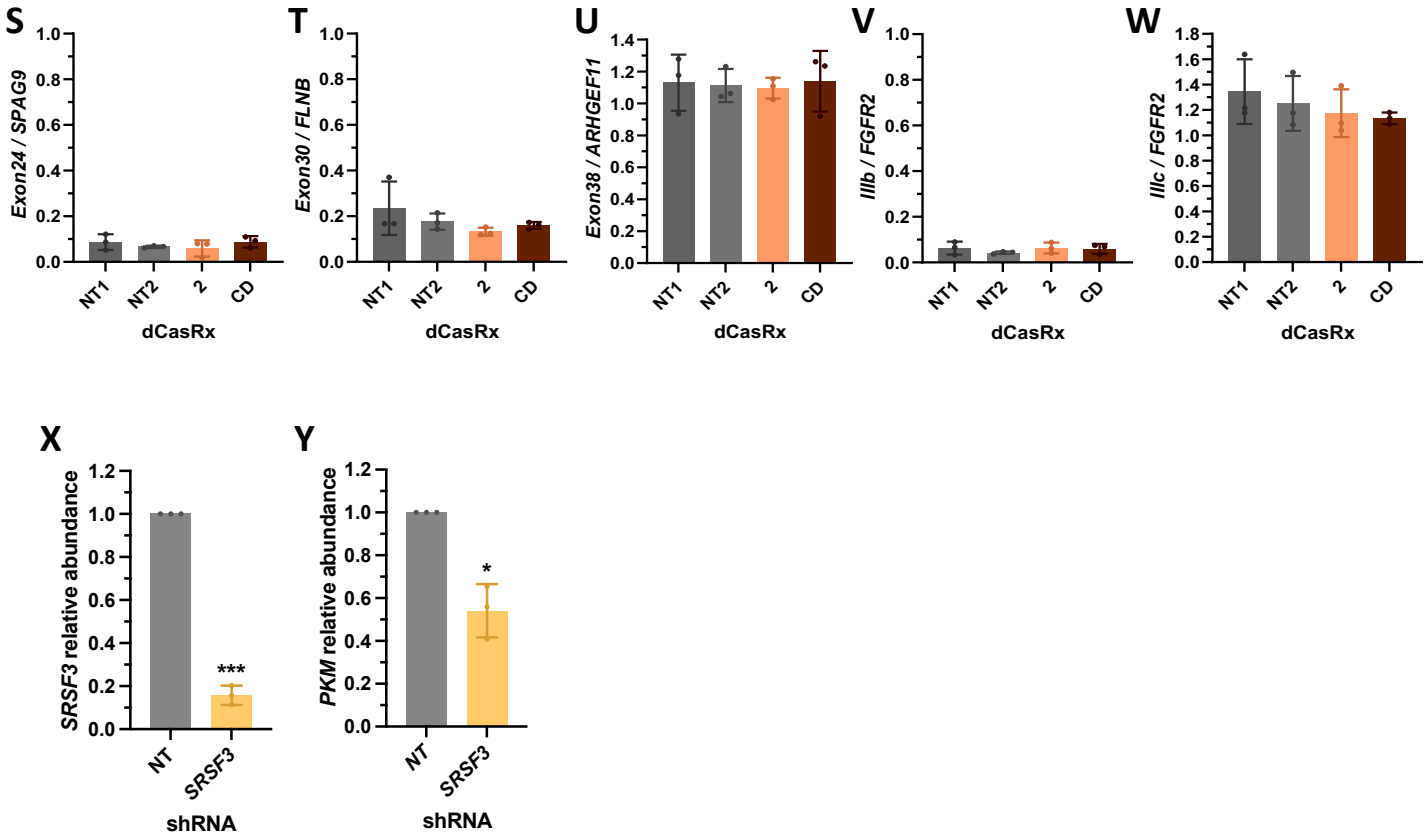

Supplementary Figure 4. dCasRx can also impact mutually exclusive exons. (**A,B**) Uncropped western blot gels from 5 biologically independent experiments corresponding to Figure 4E. HEK293T cells were transfected for 72h with 800 ng of dCasRx and 800 ng of sgRNA in 24-wells. (**C**) Quantification of PKM1 western blot bands by calculating with ImageJ software the optical density (OD) of each band and normalizing with TUBULIN's OD for every replicate in HEK293T cells transfected with dCasRx and *PKM*.ex10 gRNA CD or NT2 as control. (**D-W**) Inclusion levels of 20 alternatively spliced exons chosen randomly in HEK293T cells after 72h transfection with 200ng of dCasRx and 200ng of the indicated gRNA targeting *PKM*.ex10. RT-qPCR levels are normalized by total gene expression levels and represented as mean +/- SD in n=3 biological replicates. Despite changing *PKM*.ex 9 inclusion levels (shown in Fig.4C), these gRNAs have no off-target effect in other alternatively spliced exons. (**X-Y**) *SRSF3* knock-down efficiency (**X**) and impact on *PKM* levels (**Y**) upon shRNA-mediated *SRSF3* knock-down in HEK293T cells. RT-qPCR levels were normalized by *TBP* and non targeting shRNA NT in n=3 biological replicates. **P* <0.05, ***P* <0.01, ****P* <0.001, in two-tail not paired Student's t-test respect Non targeting shRNA (NT grey).